

Streamline Simulation

Marco R. Thiele

Streamsim Technologies, Inc.

ABSTRACT

Streamline-based flow simulation (SL) is an effective and complementary technology to more traditional flow modeling approaches such as finite differences (FD). This is because streamline-based flow simulation is particularly effective in solving large, geologically complex and heterogeneous systems, where fluid flow is dictated by well positions and rates, rock properties (permeability, porosity, and fault distributions), fluid mobility (phase relative permeabilities and viscosities), gravity, and voidage replacement ratios close to one. These are the class of problems more traditional modeling techniques have difficulties with. More diffusive mechanisms, such as capillary pressure effects and expansion-dominated flow, on the other hand, are not modeled efficiently and accurately by streamlines.

Modern SL simulation rests on 6 key principles: (1) tracing three-dimensional (3D) streamlines in terms of time-of-flight (TOF); (2) recasting the mass conservation equations along streamlines in terms of TOF; (3) periodic updating of streamlines; (4) numerical 1D transport solutions along streamlines; (5) accounting for gravity effects using operator splitting; and (6) extension to compressible flow. These principles are reviewed in detail in this paper.

The application of SL simulation is presented in the context of what are generally considered important areas in reservoir engineering: (1) flood optimization; (2) history matching; (3) assessing uncertainty in reservoir performance; (4) upscaling; (5) screening of enhanced recovery projects; and (6) rapid sensitivity studies on model parameters. In addition, novel, streamline-specific data is shown to add valuable engineering insight, and offer a powerful new representation of reservoir connectivity.

Finally, the outlook for streamline-based simulation is discussed in the context future trends. The speed and efficiency as well as the availability of new data make streamlines potentially the most significant tool for solving complex optimization problems related to history matching and optimal well placements.

Streamline Simulation	1
<i>Abstract</i>	<i>1</i>
<i>Historical Context & The Six Key Ideas</i>	<i>3</i>
Key Idea #1: Tracing Streamlines in Three Dimensions Using Time-of-Flight	4
Key Idea #2: Recasting the mass conservation equations in terms of time-of-flight.	7
Key Idea #3: Periodic updating of streamlines.	8
Key Idea #4: Numerical solutions along streamlines	9
Key Idea #5: Gravity.	10
Key Idea #6: Compressible Flow	11
<i>Why Streamline-Based Simulation is Successful</i>	<i>14</i>
Flow Visualization	14
Efficiency and Computational Speed	15
Full Field Modeling vs. Sector Modeling	18
Flow Physics—Starting with the Simplest Model	19
Incompressibility and Well Controls	20
Novel Engineering Data	21
<i>Applications of Streamline Simulation</i>	<i>22</i>
Waterflood Optimization	22
Pattern Balancing	25
History Matching	30
Ranking & Uncertainty in Reservoir Performance	34
Upscaling and Streamlines	36
Miscible Flooding Using Streamlines	39
<i>Moving Forward With Streamline Simulation</i>	<i>41</i>
Compositional Simulation	41
Tracing Streamline Through Structurally Complex Reservoirs	42
Streamlines in Fractured Systems	42
Simulation of Large System	42
New Work Flows	42
<i>The Future Simulator</i>	<i>42</i>
<i>Acknowledgments</i>	<i>43</i>
<i>References</i>	<i>43</i>

HISTORICAL CONTEXT & THE SIX KEY IDEAS

The current popularity of SL simulation should more aptly be termed a resurgence, given that streamlines—as pertaining to modeling subsurface fluid flow and transport—have been in the petroleum literature since Muskat and Wyckoff’s 1934 paper and have received repeated attention since then. It is not the author’s intention to give a full review of the technology in this paper. The interested reader is referred to the many papers and dissertations having extensive discussions and reference lists.

Suffice to say that the classical approach to modeling streamlines was to use the line source solution and the principle of superposition in two dimensions (2D) under the assumptions of incompressibility, unit mobility ratio, and a homogenous and isotropic reservoir to derive the flux vectors (Caudle 1966)

$$\begin{aligned} v_x &= \frac{1}{2\pi h \phi} \sum_{i=1}^m q_i \frac{(x-x_i)}{(x-x_i)^2 + (y-y_i)^2} \\ v_y &= \frac{1}{2\pi h \phi} \sum_{i=1}^m q_i \frac{(y-y_i)}{(x-x_i)^2 + (y-y_i)^2} \end{aligned} \quad (1)$$

where m is the number of sources or sinks, including image wells, and q_i is the (constant) volumetric rate of the source (+) or sink (-) located at (x_i, y_i) . The streamlines could then easily be traced from source to sink by using an explicit integration

$$x^{n+1} = x^n + (t^{n+1} - t^n) \times v_x|_{x^n, y^n} \quad ; \quad y^{n+1} = y^n + (t^{n+1} - t^n) \times v_y|_{x^n, y^n} \quad (2)$$

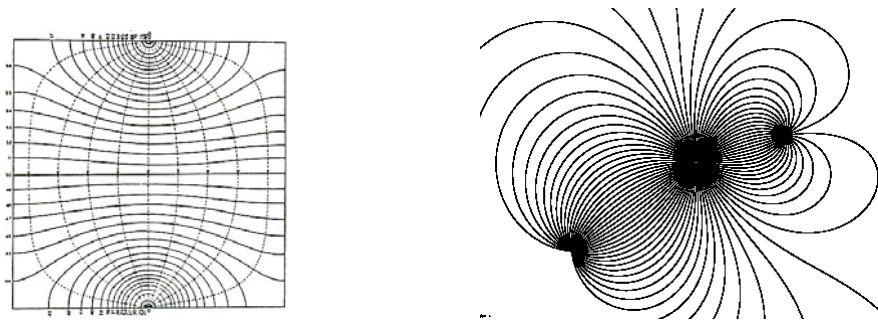


Figure 1: (Left) Streamlines and iso-potential lines for a direct line drive from Muskat and Wyckoff’s 1934 paper “A Theoretical Analysis of Water-Flooding Network”; (Right) Streamlines derived using the steady state line source solution and the principle of superposition for an infinite reservoir from B. Caudle’s SPE Lecture Notes (1966) on Reservoir Engineering.

Though helpful for basic reservoir engineering analysis, using streamlines derived using the assumptions inherent in the line source solution became too restrictive, particularly when compared to the emerging finite-difference alternative that offered a more general approach to track fluid movement in geologically heterogeneous systems. Since then, streamline based simulation has resurfaced thanks to six key ideas that form the core of the current state-of-the-art of the technology.

Key Idea #1: Tracing Streamlines in Three Dimensions Using Time-of-Flight

One distinguishing feature of current SL simulation is that the streamlines are truly 3D, rather than 2D as in the streamline and streamtube methods of the 70's and 80's. While streamlines are generally depicted from a birds-eye perspective, streamlines now correctly account for the previously missing third (vertical) flow component. Adding the third dimension has been critical to the current success of the technology, capturing cross-flow between layers and flow around geological barriers, and most importantly: gravity. From a practical point of view, the availability of 3D streamlines no longer requires geological models to be transformed into pseudo 2D areal homogenous models. Instead, models can retain a full 3D, geocellular description, and streamlines can appear crossing in a 2D plan view—as in Figure 2—because of the added dimensionality of the problem.

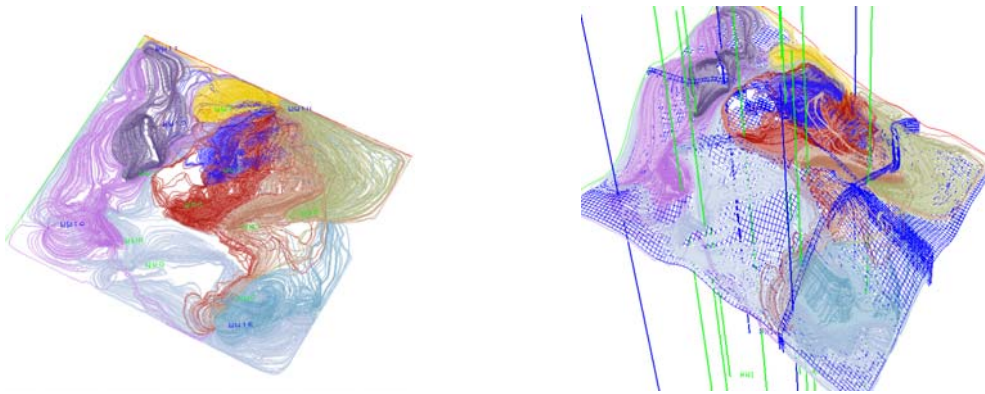


Figure 2: Although SL are generally depicted from a birds-eye perspective and appear 2-dimensional (left), SL's today are truly 3D and properly account for the vertical flow component (right).

The breakthrough work for tracing streamlines efficiently in 3D was that of Pollock (1988). Pollock's method is simple, analytical, and is formulated in terms of a time-of-flight (TOF) coordinate. To apply Pollock's tracing method to any cell, the total flux in and out of each boundary is calculated using Darcy's Law. With the flux known, the algorithm centers on determining the exit point of a streamline and the time to exit given any entry point assuming a piece-wise linear approximation of the velocity field in each coordinate direction. This is consistent with the assumptions inherent in the 7-point stencil used in finite-differencing.

The equations are simple: if v is the interstitial velocity ($v=u/\phi$), then a linear, independent velocity description in the x-direction gives

$$v_x = v_{x0} + g_x(x - x_0); \quad g_x = \frac{v_{x+\Delta x} - v_{x0}}{\Delta x} \quad (3.)$$

where v_{x0} is the x-velocity at $x=x_0$, and g_x is the velocity gradient in the x-direction (Figure 3).

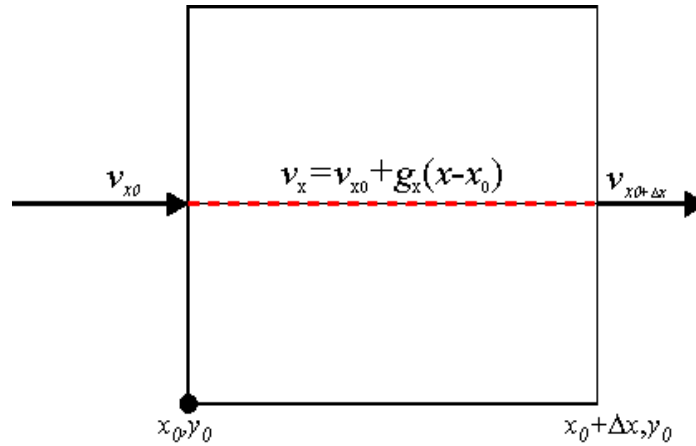


Figure 3: Pollock’s methods uses a linear velocity description in each coordinate direction.

Since $v_x = dx/dt$, Eq.(3.) can be integrated (and in analogous fashion in the y- and z-direction) to determine the time it takes to exit from each possible face. In other words, given an entry point (x_i, y_i, z_i) , the times associated with exiting from each of the three possible faces (x_e, y_i, z_i) , (x_i, y_e, z_i) , and (x_i, y_i, z_e) are given by

$$\Delta t_x = \frac{1}{g_x} \ln \left[\frac{v_{x0} + g_x(x_e - x_0)}{v_{x0} + g_x(x_i - x_0)} \right]$$

$$\Delta t_y = \frac{1}{g_y} \ln \left[\frac{v_{y0} + g_y(y_e - y_0)}{v_{y0} + g_y(y_i - y_0)} \right]$$

$$\Delta t_z = \frac{1}{g_z} \ln \left[\frac{v_{z0} + g_z(z_e - z_0)}{v_{z0} + g_z(z_i - z_0)} \right]$$

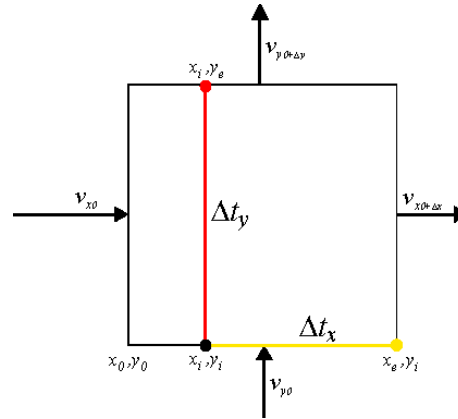


Figure 4: The linear velocity model in each coordinate direction allows to determine the time it takes for a particle to exit in each coordinate direction given the entry point (x_i, y_i, z_i) .

Since the streamline will exit from the face having the smallest travel time, $\Delta t_{min} = \text{MIN}(\Delta t_x, \Delta t_y, \Delta t_z)$, the exit location can be calculated using the minimum travel time through the cell and solving the equations in reverse gives the exit coordinates:

$$\Delta t_m = \text{MIN}(\Delta t_x, \Delta t_y, \Delta t_z)$$

$$x_e = \frac{1}{g_x} [v_{xi} \exp(g_x \Delta t_m) - v_{x0}] + x_0$$

$$y_e = \frac{1}{g_y} [v_{yi} \exp(g_y \Delta t_m) - v_{y0}] + y_0$$

$$z_e = \frac{1}{g_z} [v_{zi} \exp(g_z \Delta t_m) - v_{z0}] + z_0$$

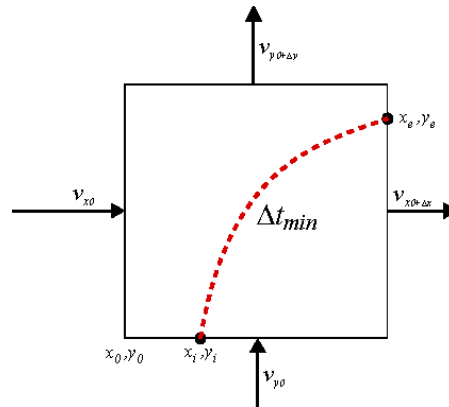


Figure 5: Pollock’s 3D tracing method through a Cartesian cell. The minimum travel time is used to find the exit point (x_e, y_e, z_e) given an arbitrary entry point (x_i, y_i, z_i) .

Once the exit point location (x_e, y_e, z_e) is known, it becomes the inlet position of the neighboring block and so the streamline can be traced from block to block as shown in Figure 6.

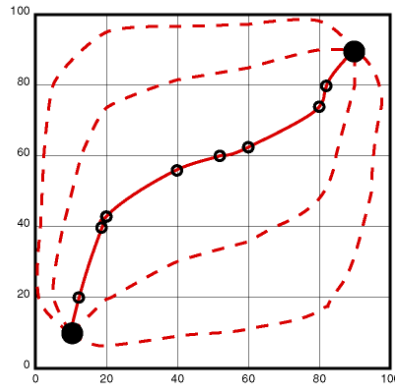


Figure 6: (Left). Given an arbitrary entry point, the time to exit and the exit point can be determined analytically (Pollock 1988). (Right) The exit point of one cell becomes the entry point for the next cell. By connecting exit and entry points a streamline is traced from injector to producer.

Pollock’s equations assume orthogonal grid blocks and a linearly independent velocity model, yet few real reservoirs models use such a strict Cartesian framework anymore. Using an isoparametric transformation, it is possible to transform corner-point geometry grids (CPG) into unit cubes, apply Pollock’s method, and then transform the exit coordinate back to physical space. One such approach is given by Cordes & Kinzelbach (1994) and by Prevost et al. (2002). Using Pollock’s method and modifications thereof it is possible to trace streamlines through any realistic grids, including unstructured grids, used in reservoir simulation (Prevost et al. 2002).

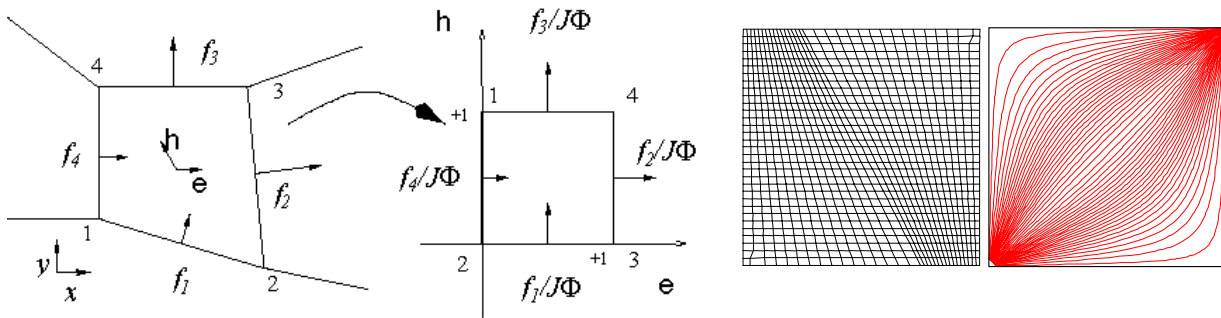


Figure 7: (Left) Non-orthogonal cells can be transformed using an isoparametric transformation. Pollock’s method can then be applied to the resulting unit cell (from Prevost et al. 2002). (Right) Streamlines in a homogenous 5-spot using a non-orthogonal grid and an isoparametric transformation (from Prevost et al. 2002).

Given Pollock tracing algorithm, the natural extension of the 2D streamtube approaches of the 70’s and 80’s would appear to be the definition of 3D streamtubes. However, keeping track of geometrical objects in 3D is a cumbersome and numerically expensive proposition. A simpler and more efficient approach is to consider every streamline as the center of a streamtube whose volume is known— $\Delta V = Q_t \Delta \tau$ —but whose boundaries are not. Here, Q_t is the total flow rate and $\Delta \tau$ is the delta TOF required to cross the gridblock. Thus, streamlines with small TOFs are equivalent to streamtubes with small volumes, i.e. fast flow regions. Conversely, streamlines with large TOFs

are equivalent to streamtubes with large volumes, i.e. slower flow regions. Reformulating the transport problem along a streamline using TOF—rather than along a streamtube using volume—is the one key innovation that has allowed SL flow simulation to succeed for use in complex, 3D problems.

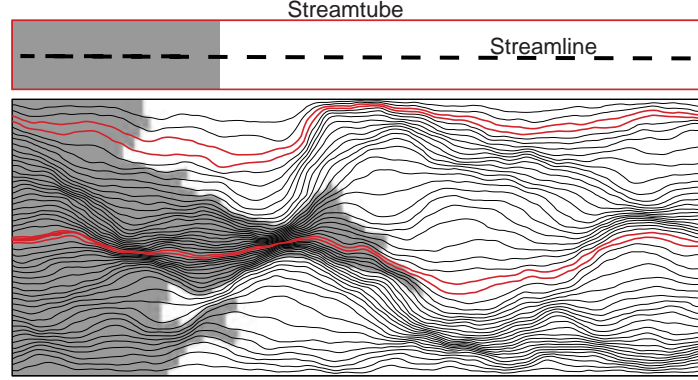


Figure 8: Filling a streamtube with a given volume is equivalent to walking the center streamline of the tube to a given time-of-flight (from Thiele et al., 1996).

Key Idea #2: Recasting the mass conservation equations in terms of time-of-flight.

The understanding that using a TOF-variable along streamlines rather than a volume-variable along streamtubes came through the reformulation of the 3D mass conservation equations in terms of TOF. This was first shown by King et al. (1993) and later expanded on by Datta-Gupta and King (1995). The central assumption in the derivation was that the streamlines did not change over time—an assumption later relaxed as described in the next section. The derivation is simple (Blunt et al., 1996, Batycky et al. 1997, Ingebrigtsen et al. 1999). For incompressible and immiscible flow without gravity, the conservation equation for a phase j can be written as

$$\phi \frac{\partial S_j}{\partial t} + \bar{v}_t \cdot \nabla f_j = 0 \quad (4.)$$

where S_j is the saturation of phase j , $\bar{v}_t = \sum \bar{v}_j$ is the total velocity and f_j is the fractional flow of phase j . Consider the definition of the TOF, which is just the time it takes a particle to travel a given distance along a streamline having a total velocity of magnitude $|\bar{v}_t|$ defined along it. Thus,

$$\tau = \int \frac{\phi}{|\bar{v}_t|} d\xi \quad \rightarrow \quad \frac{\partial \tau}{\partial \xi} = \frac{\phi}{|\bar{v}_t|} \quad \rightarrow \quad |\bar{v}_t| \frac{\partial}{\partial \xi} = \phi \frac{\partial}{\partial \tau} \quad (5.)$$

But notice that along a streamline

$$\bar{v}_t \cdot \nabla = |\bar{v}_t| \frac{\partial}{\partial \xi} \quad (6.)$$

which allows the 3D conservation equation to be re-written as a 1D equation along streamlines in terms of TOF:

$$\frac{\partial S_j}{\partial t} + \frac{\partial f_j}{\partial \tau} = 0 \quad (7.)$$

There are a number of assumptions buried in this derivation: (i) the volumetric flowrate along each streamline is assumed constant; (ii) the streamlines do not change over time (steady state flow); and (iii) the 1D solutions must have the same boundary and initial conditions as the 3D problem. What the derivation does show though, is that a three-dimensional transport problem can be re-written in terms a sum of one-dimensional problems along streamlines. While this was known intuitively from the work on streamtubes, the TOF formulation offers a compelling and clear mathematical framework. For the simple case of an incompressible waterflood it is thus possible to write

$$\phi \frac{\partial S_j}{\partial t} + \bar{u}_i \cdot \nabla f_j = 0 = \sum_{\text{streamlines}}^{\text{all}} \left(\frac{\partial S_j}{\partial t} + \frac{\partial f_j}{\partial \tau} \right) \quad (8.)$$

The most important detail about Eq.(8.) is that the total interstitial velocity (containing permeability and porosity) of the 3D problem has disappeared into the TOF of each individual streamline. It is this decoupling of a 3D heterogeneous system into a series of 1D homogenous systems in terms of TOF that makes the SL method so attractive.

Key Idea #3: Periodic updating of streamlines.

The fixed streamtube assumption (steady state flow) was probably the single most significant drawback that prevented a wider use of the technology during the 70's and 80's. Martin & Wegner (1979) and Renard (1990) did consider changing streamline and streamtube geometries with time, but it was not until the mid 90's that the fixed-streamline assumption was relaxed for good (Thiele *et al.* 1996, Batycky *et al.* 1997). At the time, the main interest was to properly account for the rapidly changing mobility field in miscible gas injection problems. The real benefit though was that now changing reservoir conditions—changing flow rates, new wells coming online, and old wells being shut in—and gravity could also be accounted for.

The idea was to treat the problem as a succession of steady-states by considering each updated streamline field valid only for a fixed time interval before updating it. The method worked well for mobility induced nonlinear problems, but mapping analytical, self-similar hyperbolic solutions (Thiele *et al.* 1995, 1997) would not allow to solve systems with changing well conditions and gravity, due to the requirement of uniform initial conditions along streamlines imposed by the analytical solutions. One additional element was needed: the ability to solve transport problems with generalized initial conditions along each streamlines (Batycky *et al.* 1997). Streamline geometries could then change at will, guaranteeing that fluids would be transported in the correct directions by having initial compositions picked-up from their position at the end of the previous timestep.

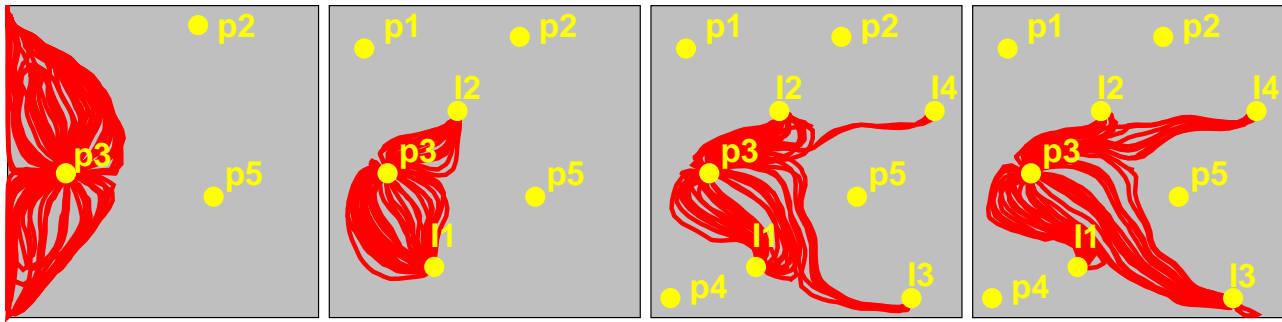


Figure 9: Streamline geometries can change due to changing well conditions—i.e. rate changes, new wells coming online, or wells being shut-in—as well as a changing mobility field. In general, changing wells conditions will have a stronger impact on streamlines geometries that changes in the mobility field alone.

Key Idea #4: Numerical solutions along streamlines

Numerical 1D solutions along streamlines were first introduced by *Bommer & Schechter (1979)* to solve a Uranium leaching problem. In their work, *Bommer & Schechter* used fixed streamlines (steady state) but a numerical solution was used to solve the transport problem along each streamline because there was no analytical solution for the problem they were interested in. *Batycky et al. (1997)* now combined changing three-dimensional streamlines with a general, one-dimensional, numerical solution in TOF-space. This merging of ideas was instrumental in allowing streamline-based simulation to be used in real field cases, where streamlines would not only change due to mobility differences but also because of changing well conditions. With every new set of streamlines, the correct initial conditions could be mapped onto the streamlines—i.e. the conditions existing at the end of the previous timestep—and moved forward in time numerically. This allowed moving components correctly in 3D despite significant and radical changes in streamline geometries due to changing well conditions. Using 1D numerical solutions also made it possible to consider any 1D solution along streamlines, including complex compositional displacements (*Thiele et al. 1997*) or multi-component contaminant transport in aquifers (*Crane and Blunt 2000*). More recently, the solution for dual-porosity models has also been solved along streamlines (*Di Donato et al. 2003, Di Donato & Blunt 2004, Thiele et al. 2004*).

One noteworthy issue arising from treating streamlines as discrete 1D systems is that the resulting discretization in TOF-space will result in a very irregular 1D grid, possibly with orders of magnitude differences between the smallest and largest cell. To maintain overall computational efficiency, it is imperative that a reasonable ratio between the smallest and largest cell along the streamlines be maintained. The approach used initially by *Batycky et al. (1997)* was to use a regular discretization of the original TOF grid along each streamline. Using a sufficient amount of nodes (50-100) would guarantee an accurate representation of the solution, reduce the mixing of fluids resulting from the regularization, and ensure an efficient solution of the hyperbolic transport equations. More recent applications (*3DSL 2003*) have moved away from the regular grid in favor of an irregular grid in which only the smallest cells are eliminated and merged with its neighbors. This approach avoids the unnecessary mixing between all cells that is caused in the regularization approach, yet eliminates the smallest volume cells that might trigger an excessively small throughput limit in the 1D solver.

The issue of “binning” small volume cells away has become even more significant in the context of dual-porosity systems (*Thiele et al., 2004*) in which single porosity and dual-porosity cells might co-exist in the reservoir. Cell volumes along streamlines representing the flowing fracture medium

can be order of magnitude smaller than cell volumes representing the flowing matrix medium, and therefore represent a real challenge when solving the transport equations. Although an adaptive-implicit approach can mitigate the impact of the smaller cells, convergence issues in the 1D solver will invariably require the elimination of the smallest cells through a binning approach.

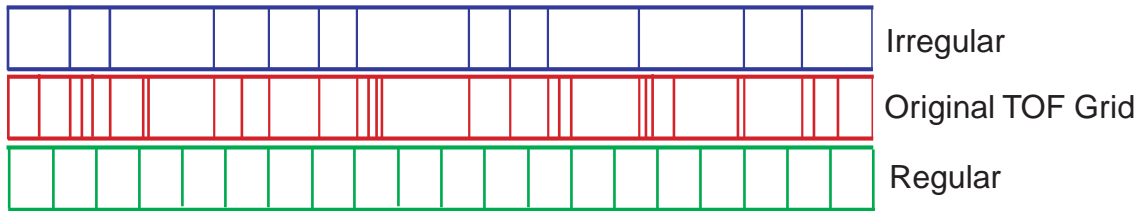


Figure 10: The 1D time-of-flight grid along each streamline will be highly irregular for all but the most simple cases. Very small cells will co-exist with large cells thereby severely restricting the throughput of the 1D solver and reducing its efficiency. To eliminate the difference between small and large cells, the original TOF grid (red) can either be regularized (green) or left on an irregular spacing while binning smaller cells into larger ones (blue).

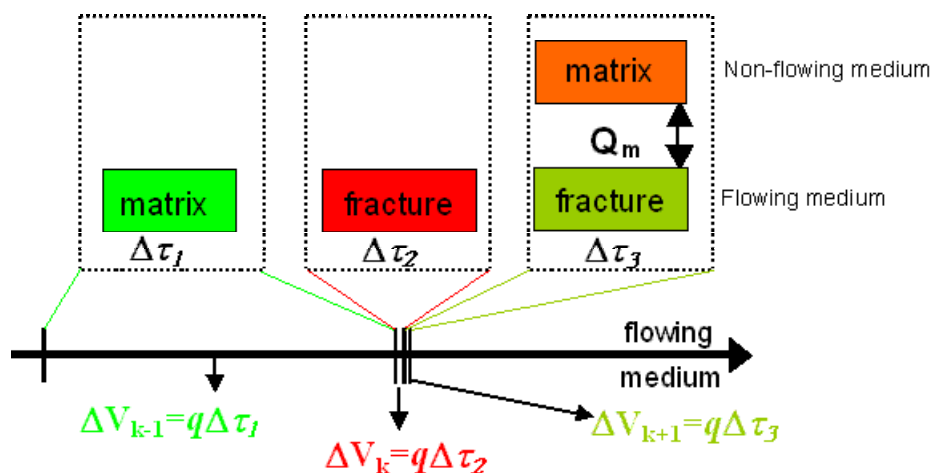


Figure 11: In the case of dual-porosity systems, the TOF grid along a streamline will invariably result in an irregular grid that has even larger differences between smallest and largest cells. An adaptive-implicit formulation will not be able to fully resolve the throughput constraint caused by the smallest cells due possible convergence issues. Binning the smallest cells away remains the best approach (from Thiele et al. 2004).

Key Idea #5: Gravity.

Including gravity in streamline simulation presented a problem. The total velocity vector—to which a streamline is tangent to—is the sum of the phase vectors. In the presence of gravity though, the phase vectors are not aligned. A solution to this problem was presented by Bratvedt et al. (1996) using the concept of operator splitting, an idea that had found previous application in front tracking (Glimm et al. 1983, Bratvedt et al. 1992) and is a well-accepted mathematical technique. Operator splitting solves the material balance equations in two steps: first a “convective step” is taken along the streamlines which is then followed by a “gravity” step along gravity lines—lines

parallel to the gravity vector \vec{g} . In the gravity step fluids are segregated vertically according to their phase densities only. This is not to be confused with a vertical equilibration problem.

The mathematics is rather simple. The conservation equation for incompressible, immiscible flow can be written as

$$\frac{\partial S_j}{\partial t} + \frac{\partial f_j}{\partial \tau} + \frac{1}{\phi} \frac{\partial G_j(S_j)}{\partial z} = 0; \tag{9}$$

$$G_j(S_j) = f_j \sum_{i=1}^{n_p} \lambda_i (\rho_i - \rho_j); \quad f_j = \frac{|u_j|}{\sum |u_i|}$$

Operator splitting solves the conservation equation by breaking it up into two, in which the solution of the first part becomes the initial conditions for the next.

$$\frac{\partial S_j}{\partial t} + \frac{\partial f_j}{\partial \tau} = 0; \tag{10}$$

$$\frac{\partial S_j}{\partial t} + \frac{1}{\phi} \frac{\partial G(S_j)}{\partial z} = 0$$

While the order of the solution is mathematically immaterial, streamline-based simulation solves the convective step first followed by the gravity step.

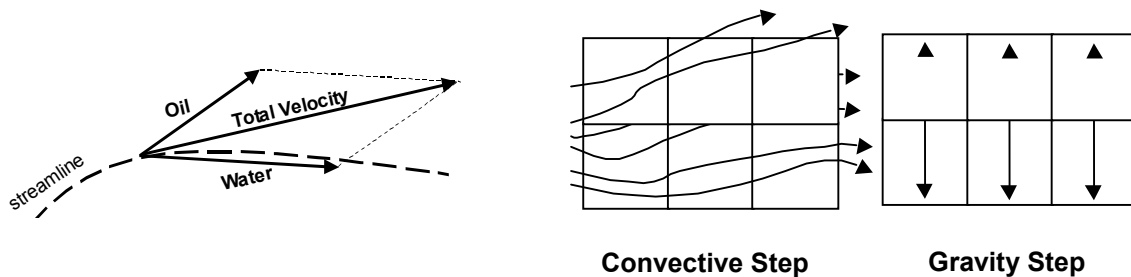


Figure 12: In the presence of gravity, the phase velocity vectors are not aligned with the total velocity vector defining the streamline. Thus, moving components along the total velocity for multiphase flow will not account for gravity segregation. This is corrected using an operator splitting approach.

Key Idea #6: Compressible Flow

All streamtube and streamline work in the past was restricted to the assumption of incompressible flow. The reason, of course, is that incompressible flow introduces simplifying assumptions that are particularly suitable for SL simulation. Two assumptions in particular are worth mentioning:

1. source and sinks correspond to wells (or an aquifer), meaning that all streamlines must start in a source (an injector) and end in a sink (producer); and
2. the flow rate along each streamline (or streamtube) is constant.

This second assumption is particularly important as it implies that transport along a streamline only involves solving for the component wave speeds, and is completely independent of the absolute pressure level. The absolute pressure level is immaterial in the incompressible formulation.

The problem for streamline simulation, of course, is that there are no real incompressible systems: all field cases involve compressible flow characteristics to some extent. PVT properties can and usually are a strong function of pressure, as in black-oil or gas condensate systems, and the voidage replacement ratios (reservoir volume in/reservoir volume out) can deviate significantly from unity, either locally or on a field wide basis leading to significant pressure changes.

If the flow is compressible then streamlines can start or end in any gridblocks that act as a source or sink, even if the block has no well. For example, in expansion type problems, any gridblock that sees its volume increase with decreasing pressure is a source and thus a potential starting point for a streamline.

Figure 13 shows streamlines under primary depletion. Streamlines now start in the far field and end in producers that act as sinks, yet there are no ‘real’ sources (injection wells) in the traditional sense. Instead, the sources are all along each streamline, since every gridblock a streamline passes through now acts as a source due the fluid expansion.

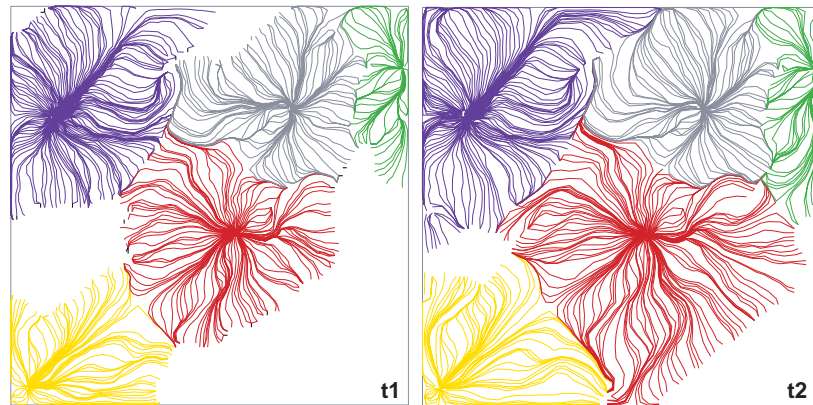


Figure 13: Streamlines shown at two different times during primary depletion. In compressible flow, gridblocks act as sources even though there are no injection wells. A streamline will start in the far field and end in a producer collecting volumes from each gridblock it crosses.

Determining and tracing streamlines in compressible flow is not difficult. Pollock’s tracing algorithm is valid regardless of how the flow velocities are determined so long as the linear independence in each coordinate direction is maintained, and the TOF automatically reflects the effects of compressibility as the velocity field is determined from a compressible formulation in the first place.

But a significant extension to the mathematical formulation is required to account for the coupling between saturations/compositions and pressure that now exists along the streamlines. There is also the additional complication that the flow rate is no longer constant along the streamline. One possible solution has been published by Ingebrigtsen et al (1999). A different, un-published approach has been implemented into a commercially available code (3DSL 2003) and used for modeling compressible immiscible and miscible three-phase systems.

But while streamlines can model truly compressible systems, the inherent speed advantage over FD methods can diminish significantly depending on model size and governing displacement mechanisms. This is due simply to the constraint that if absolute pressure needs to be properly

resolved to capture the pressure transients, then limits on the global timestep size become very similar to FD methods. However, there are examples where compressible SL solutions are still the only possible method to simulate very large secondary and tertiary displacement processes in a reasonable amount of time on off-the-shelf computing resources.

If PVT properties are only a weak function of pressure, the incompressible framework can still be used successfully to model compressible systems through the introduction of “open” reservoir boundaries. Open boundaries can be distributed anywhere on the edges of the simulation model, with each boundary cell set to a constant pressure thus ensuring exact voidage replacement as required by the incompressible formulation. The approach works well. Streamlines originating from the boundaries mimic the flow from the far field that would be observed in a closed but compressible system. Production profiles show similarly good comparison. The advantage with this approach is that historical injection/production volumes on a per well basis are honored exactly while the speed and efficiency of the incompressible formulation is retained.

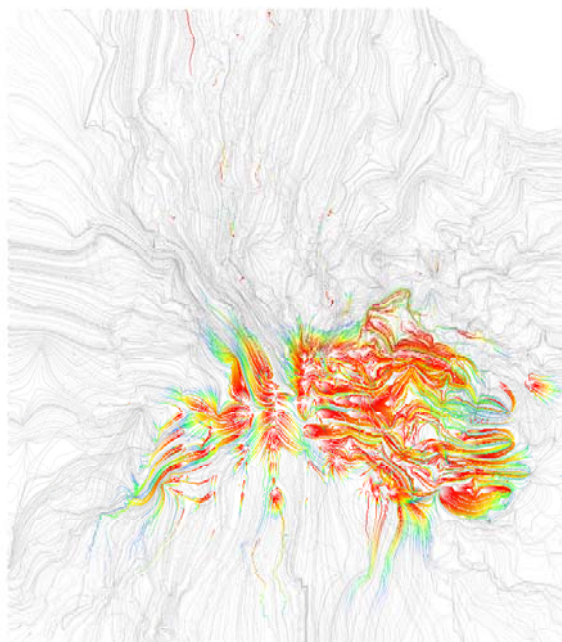


Figure 14: Open boundaries allow to model systems with non-unit voidage replacement ratio and PVT properties that are a weak function of pressure in incompressible mode, while honoring historical injection/production well volumes. The coloring of the streamlines is based on TOF, with red showing smaller TOF than gray. The model has “open boundaries” on all 4 sides.

The previous six key ideas are central to the current state of SL simulation. Many mathematical details have been left out in the interest of time and clarity, but the curious reader will find many of the publications referenced to be excellent sources. For a comprehensive source of how streamline simulation came into being and many additional details, the reader is referred to Rod Batycky’s in-depth PhD Thesis (1997).

WHY STREAMLINE-BASED SIMULATION IS SUCCESSFUL

A number of papers have clearly shown the applicability of SL simulation to solve reservoir engineering problems that have traditionally been difficult to model with more conventional techniques. In particular, near incompressible displacements (waterfloods) in large, heterogeneous earth models. Rather than re-iterating the numerous examples and conclusions in the literature, the question as to why streamline-based simulation has been so successful and has so quickly re-surfaced as a powerful alternative to more classical simulation techniques is addressed here. This question was also considered by Baker et al. (2001).

Flow Visualization

The single most attractive feature of SL simulation for many engineers is the visual power of streamlines in outlining flow patterns. Streamlines offer an immediate snapshot of the flow field clearly showing how wells, reservoir geometry, and reservoir heterogeneity interact to dictate where flow is coming from (injectors) and going to (producers). The ability to see the entire flow field at once is powerful, and invariably yields unexpected and surprising flow behavior of the model under consideration. Real fields, even those drilled in regular patterns, rarely show streamlines conforming to the expected distribution of fluids, and it is not unusual to see wells communicating with other wells far outside the expected pattern.

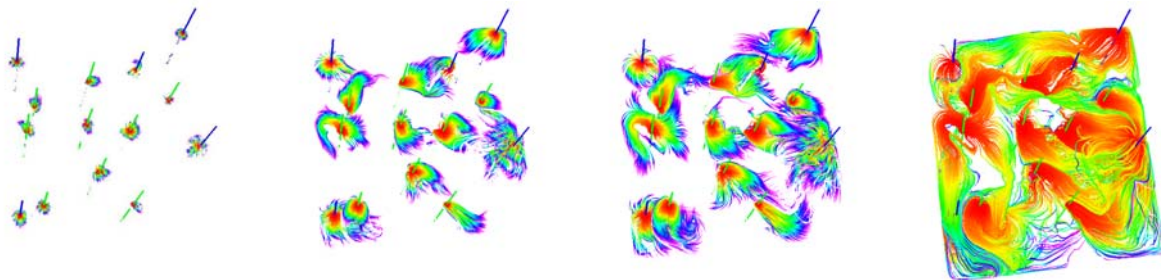


Figure 15: Streamlines can capture in a visually appealing way how sweep/drainage areas associated with injectors (blue) and producers (green) grow with time (left to right). In this picture, the streamlines are kept fixed and are colored by TOF/DRT with an increasing time scale. The left most picture shows the volume associated with a TOF/DRT cutoff of 1 year, the right most picture the volume associated with a TOF/DRT cutoff of 20 years.

The visualization can be enhanced by considering different coloring schemes of the streamlines. Coloring by TOF, or drainage time (DRT), with different cutoffs can vividly capture the growth of the swept/drainage areas over time.

The connectivity of the reservoir that is expressed by the streamlines can also be abstracted into a Flux Pattern Map (FPmap), which is what most reservoir engineers intuitively understand is being expressed by the streamlines. The FPmap is a schematic display of how injectors and producers are connected as a result of field rates, geological constraints, and flow physics, and is obtained by collapsing all the streamlines between a well pair into a single straight line connection. The FPmap is a powerful representation because it highlights data of particular interest to reservoir engineers:

1. What type of pattern flow exists in the field; and

2. What is the volumetric rate associated with an injector/producer pair.

As shown later, the FPmap is a good example of how streamlines are able to complement more traditional finite difference simulation by supplying novel information and lead to new and powerful reservoir engineering workflows, such as waterflood optimization (Thiele & Batycky, 2003).

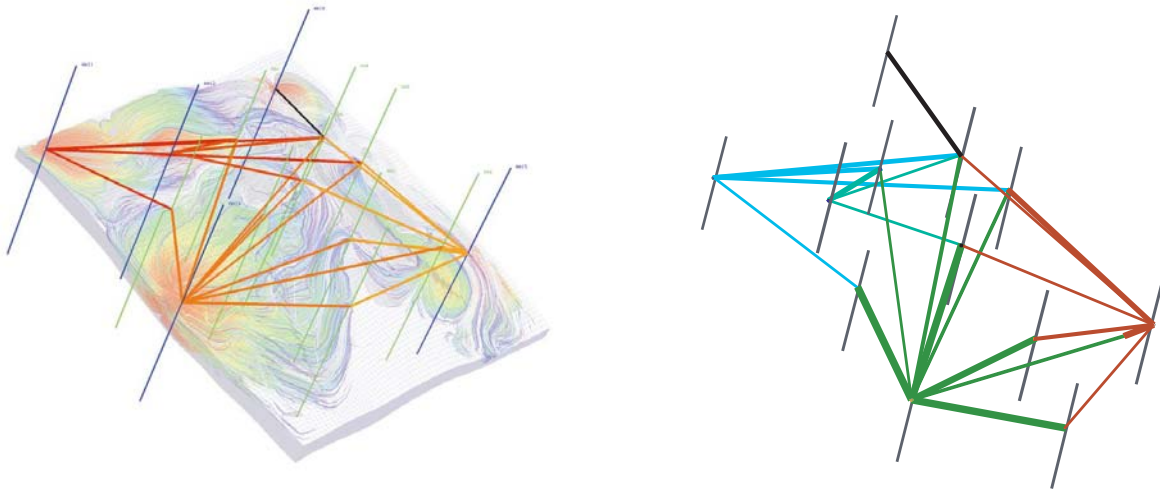


Figure 16: (Left) The Flux Pattern Map (FPmap) is a powerful abstraction of information supplied by streamlines. (Right) It more readily shows the injector/producer pairs (green injector is supporting 8 producers) and line thickness' can be related to the flux between the well pairs.

Efficiency and Computational Speed

Computational speed and efficiency are often mentioned as one of the key advantages of SL simulation over more traditional simulation approaches. However, the efficiency comes at a price: simplified flow physics and a non-mass conservative formulation among other assumptions. For many real fields, the efficiency and speed of SL simulation offers the opportunity to solve outstanding engineering queries that might otherwise be addressed only with difficulty—if at all—using other approaches. The two most common examples are flow simulations on multi-million, geocellular models with complex heterogeneity, and repeated simulations of equally probable reservoir models to quantify sensitivities of model parameters and uncertainties in forecast predictions.

But what makes SL simulation so computationally efficient? This question is best divided into two parts: memory efficiency and computational efficiency.

Memory Efficiency

Two aspects contribute to the memory efficiency of SL simulation:

- (1) streamline-based simulation is an IMPES-type formulation and therefore involves only the implicit solution for a single variable, pressure on the global, 3D scale;
- (2) tracing of SL's and the solution of the 1D transport problem along each streamline is done sequentially, and thus only one streamline is kept in memory at any given time.

Combined with good coding practices, an efficient memory management of grid arrays, and an efficient linear solver such as Algebraic Multigrid (Stüben 2000), it is possible to run models that

use approximately 400MB per million active cells (*Samier et al., 2002*). This means that it is possible to run finely meshed models on relatively inexpensive computational platforms (PC's).

Computational Efficiency

Computational efficiency, on the other hand, is achieved because of three main characteristics of SL simulation:

- (1) The velocity field (i.e. pressure) and associated streamlines only need to be updated infrequently (large time step sizes)
- (2) The 1D transport problem along each streamline can be solved efficiently.
- (3) The number of streamlines increases linearly with the number of active cells.

Combined with an efficient matrix solver, points 1-3 above give rise to a near-linear scaling of run times with the number of active cells as shown in Figure 17 for the SPE10 comparative solution project.

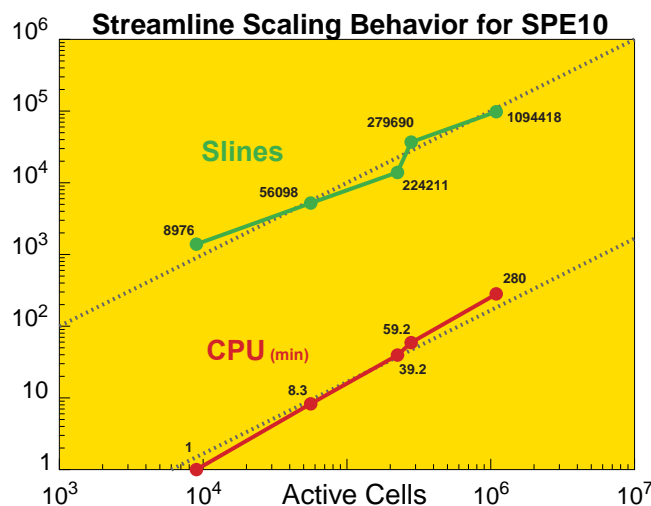


Figure 17: Example of linear scaling of run time and number of streamlines as a function of active cells for the SPE Comparative Solution Project #10 using 3DSL, a commercial streamline simulator, on a PIII 866MHz PC.

The first point—that streamlines need to be updated only infrequently—is a key ingredient for the computational efficiency of SL simulation and deserves special attention. Streamlines change over time due to mobility changes, gravity, and changing boundary conditions. However, for many practical problems, grouping well events into yearly or semi-yearly intervals and assuming that the streamlines remain unchanged over that period yields solutions that fall well within the bounds of uncertainty of the input data. As a result, SL's are particularly useful in modeling mature waterfloods, where fields with 30 to 40 year histories are successfully and routinely simulated with 1-year time steps (*Baker et al. 2002*). Most importantly, the size and number of the global time steps (frequency of streamline updates) is insensitive to the size and heterogeneity of the 3D model. For example, “increasing” the heterogeneity of a particular model will not force smaller global timesteps as might be the case for more traditional simulation techniques. In other words, there is

no local CFL-number that directly forces smaller time steps. Instead the geometry of the SL's and the TOF along the SL's automatically capture the increased heterogeneity without need for any additional refinement of the global time step.

Solution of the mass transport along each streamline can be solved efficiently provided the 1D TOF-space is regularized or binned into an irregular grid (Figure 10). Proper discretization of the 1D problem is very important. Keeping small cells along the streamline—resulting from streamlines flowing through very high flow regions near wells or cutting cell corners, for example—would slow down the 1D transport solution along the streamline in much the same way as small cells tend to slow down IMPES solutions in regular simulators.

A good example to demonstrate the efficiency of SL simulation is Model 2 of the 10th SPE comparative solution project (*Christie and Blunt, 2001*). The total run time, T , of any streamline simulation can be expressed as

$$T \propto \sum_1^{n_{ts}} \left(t^{solver} + \sum_1^{n_{sl}} t_j^{sl} \right) \quad (11.)$$

where

n_{ts} number of time steps (number of streamline updates)

t^{solver} time required to solve for the global pressure field ($Ax = b$) at each time step

n_{sl} number of streamlines at each time step

t_j^{sl} time to solve transport equation for each streamline

The near-linear scaling in computation time arises because:

1. The number of time steps (n_{ts} streamline updates) is independent of the model size, heterogeneity, and any other geometrical description of the 3D model. It is only a function of the number of well events, averaging of production/injection volumes, and the displacement physics. For the SPE10 problem in Figure 17 all cases were run with the exact same number of streamline updates (24).
2. An efficient solver (t^{solver}) for solving the linear system of equations is expected to have a near-linear behavior (*Stüben 2000*).
3. The number of streamlines (n_{sl}) tend to increase linearly with the number of grid blocks all else being equal (Figure 17).
4. The time to solve the 1D transport problem along each streamline can be made efficient by re-gridding the underlying TOF grid and choosing an optimal number of nodes along each streamline regardless of the size of the underlying 3D grid.

The near-linear behavior with model size shown in Figure 17 is the main reason why streamline simulation is so useful for simulating reservoir models at the geo-cellular scale. In FD's, finer models not only cause smaller timesteps due to smaller gridblocks but face additional timestep restrictions resulting from increased heterogeneity as finer models tend to have wider permeability and porosity distributions. The usual workaround for traditional simulation techniques is to use an implicit or adaptive-implicit formulation, but for large problems these solutions can become prohibitively expensive, both in terms of CPU time and memory.

Full Field Modeling vs. Sector Modeling

A common practice when simulating large fields is to divide the field into sectors and simulate each sector individually. However, carving out a representative piece of the model that minimizes the flux across the simulation boundaries for all times is not trivial. This problem is well known in the industry and the success of sector models strongly depends on properly estimating the flux in-and-out of the sector, or trying to use a border around the proposed sector to cushion the impact of the assumption.

The best approach, of course, is to model the entire field and allow patterns to form freely. However, full-field models can get notoriously big (in terms of number of cells), even when using a limited number of gridblocks between wells. Although SL-based flow simulation makes some simplifying assumptions to achieve computational efficiency, a full-field SL model can still be preferable over a sector model under traditional approaches, since the error introduced by choosing approximate sector boundaries can potentially be much larger and more significant than errors introduced by the simplifications of a streamline model.

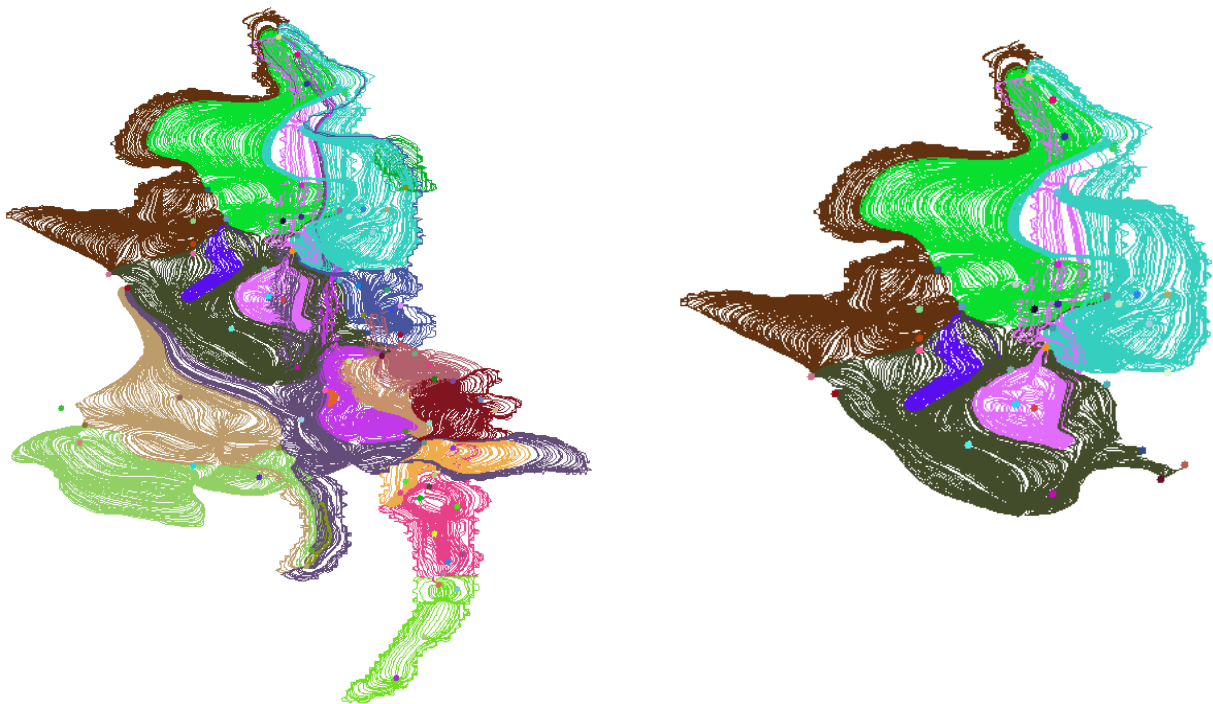


Figure 18: Example of streamlines at two different times for a full field model (streamlines colored by injectors). Carving a sector out of a full-field model is a difficult problem that can be addressed by using streamlines to find the best no-flow boundaries in the reservoir over time.

Full field vs. sector modeling is a good example of how FD's and SL are complement tools for modeling the dynamic reservoir behavior. By definition, SL's are no-flow boundaries. Therefore a streamline map could be used to identify reasonable locations for sector boundaries (Figure 18). Although streamlines do change with time, by inspecting streamline maps over time delineations of the reservoir might stand out along which it might be sensible to 'cut' the field into smaller, more manageable pieces. In this way, the errors associated with not knowing the flux across sector boundaries can be minimized.

An 80-20 Approach to Reservoir Engineering

There are significant simplifying assumptions used in SL simulation, particularly with regard to flow physics. This is because the technique grew out of an incompressible framework, with the main modeling interest being to gain insight into the field-wide reservoir flow performance, particularly as it pertains to heterogeneity interacting with injected and produced volumes. From the beginning then, the focus for SL's was on roughly capturing field displacement efficiencies, with the explicit understanding that quicker simulations on geologically more detail grids required a trade-in of more comprehensive flow physics. Streamline simulation is therefore a methodology that is inline with the classic engineering 80-20 rule where the objective is to obtain 80% of the answer in 20% of the time. How effective such an approach is has recently been presented by *Williams et al. (2004)*, where a top-down methodology—investigating the simplest possible models first and adding details later as required by business decisions—has resulted in an estimated 20% increase in net present value of the projects to which it was applied. In contrast, the all to common bottom-up strategy of using all possible information and the most detailed simulation models risks leaving the engineer overwhelmed and unable to focus on the critical engineering questions at hand.

By its very nature, SL simulation favors investigating problems using the simplest (and fastest model) first and adding increasingly complex flow physics as needed. A SL simulation study might, for example, start with inputting first order parameters such as well locations, reservoir architecture and geology, produced and injected volumes and assuming the simplest possible PVT model: single phase, incompressible flow. To introduce more complex flow physics one might then add (b) fractional flow effects using phase relative permeabilities and phase viscosities; the next step being (c) including phase density differences to account for gravitational effects; and finally (d) adding compressibility and potentially more complex phase behavior. To be fair, this natural progression of adding physical complexity to models is possible in traditional simulators as well, but it is rarely done. Instead, all too often the practice is to include as much physical complexity as the simulator allows—the “use all keywords syndrome”—and then trying to unravel the contribution of each component from the output. This bottom-up approach is no longer sustainable given the complexity and details of models that can be build and the ever-tighter budgetary and time constraints faced by engineers when making decisions.

Figure 19 shows an example of an African offshore field that was in an exploratory planning stage. The geological model size was 30x140x245 and SL quickly indicated that vertical transmissibility barriers (and thus gravity) would be an important aspect in planning well completions for insuring optimal recovery for the field. For the geologists this was a satisfactory result since it confirmed their intuitive understanding the geological description could have with numbers to back them up. More importantly, the computational efficiency of SL's allowed to screen several geological scenarios quickly—an important insight for quantifying uncertainty associated with chosen well locations. A classic 80-20 solution. The reservoir engineers, on the other hand, were preoccupied with the issue of fluid description. For this example, simulations showed that a 3 phase incompressible model was sufficient, with fluid compressibility having only a second order effect. The ratio of run times for the various models was 1: 4: 7.3 (1Phase: 3Phase Incompressible: Blackoil).

What is striking about this example is that important conclusions about the flow behavior could be determined at the early modeling stage of the field (245 simulation layers), allowing more informed engineering decisions to be made a the geo-modeling stage. A more traditional simulation approach would have likely forced some form of up-scaling risking the loss of information associated with the transmissibility barriers.

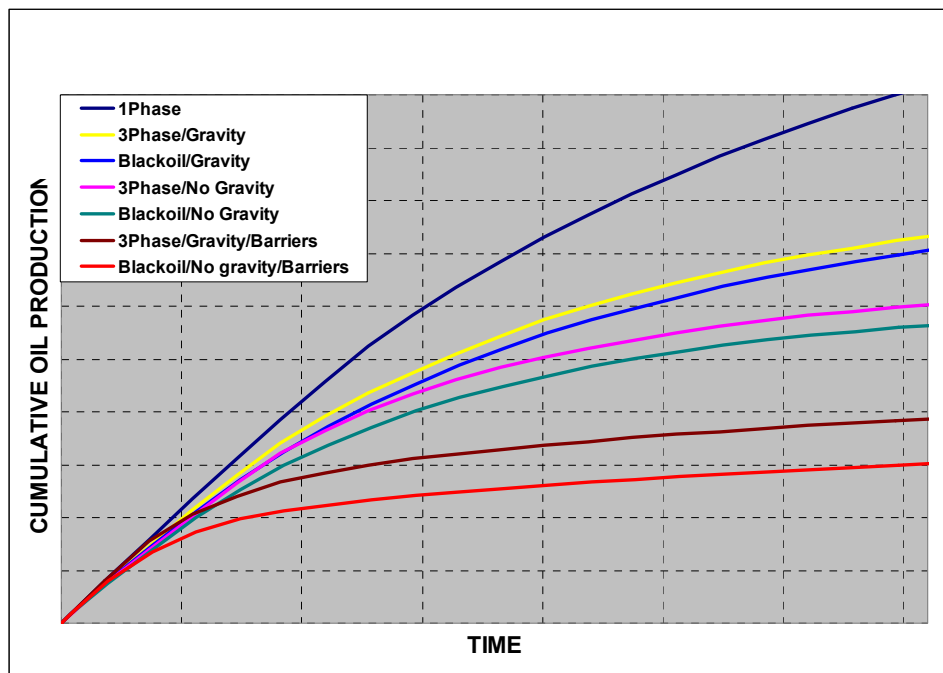


Figure 19: Streamlines offer rapid assessment of the impact of first-order flow effects on displacement efficiency. For this particular example, gravity and 3-phase flow are important aspects of the model that would have been missed using a faster but simpler single-phase flow formulation. Compressibility, on the other hand, is only of secondary importance.

Incompressibility and Well Controls

SL simulation relies heavily on the assumption of incompressibility—so much so, that it warrants its own discussion. In a truly incompressible model, the absolute pressure level is immaterial to the solution. In other words, there are no dependencies of the coefficients of the underlying partial differential equations on the absolute pressure. All that matters is the pressure gradient since it is needed in Darcy's Law to calculate the total velocity, which in turn is used to trace the SL's. By design, incompressible problems enforce an exact voidage replacement ratio of one. Though there are no real incompressible systems, many mature waterfloods, reservoirs with strong aquifer drives, and generally reservoirs being exploited above the bubble point where the primary drive energy is not supplied by fluid expansion can be modeled successfully using the assumption of incompressibility. In fact, the assumption of incompressibility can be so powerful in gaining insight into reservoir performance that it should be used whenever possible. The incompressible assumption is very much inline with a top-down engineering approach.

An attractive consequence of incompressible systems is that historical well rates can be honored exactly without having to previously ensure that the well models give physical bottom-hole flowing pressures, i.e. $P > 0$. This has important implications for history matching. Rather than starting the matching process by tuning well models to enforce historical volumes—in other words, trying to minimize the number of wells switching onto a pressure constraint—incompressible models allow the engineer to immediately begin matching the observed phase rates without regard to pressure. In fields where there are 100's, maybe 1000's of wells, it is practically impossible to honor historical well rates without allowing a good percentage of the wells to switch onto a bottom-hole-pressure constraint or even shut-in. Trying to fine-tune each well can be a painstakingly slow and costly exercise, which is made even more unnecessary in light of the fact that pressure might itself be of secondary importance in mature waterfloods. The ability to honor inter-pattern flow and generate novel, streamline-specific data, make history matching large, multi-well models a particularly well

suited problem for SL simulation. The immediate consequences are overall better field and well matches obtained in significantly less time.

Novel Engineering Data

Streamlines go well beyond their visual appeal (Figure 15) by producing new engineering data not available from conventional simulation approaches. Producing novel engineering data is potentially the most interesting and valuable contribution of streamlines to the area of reservoir engineering.

Since streamlines start at a source and end in a sink, it is possible, for example, to determine which injectors (or part of an aquifer) are supporting a particular producer, and exactly by how much. A high watercut in a producing well can therefore be traced back to specific injection wells or aquifer influx. Conversely, it is possible to determine just how much volume from a particular injection well is contributing to the producers it is supporting—particularly valuable information when trying to balance patterns. In the past, this type of well allocation data has been generated by “eye balling” rates, using isobaric maps, and the spatial vicinity of injector/producer pairs as a measure of connectedness—classic reservoir surveillance techniques. With SL simulation, the calculation of which well pairs are connected is automatic and more over accounts for the underlying geological model, a key ingredient to properly predicting reservoir performance.

Streamlines also yield drainage volumes associated with producers or irrigation volumes associated with injectors. This data is generated automatically as part of the tracing of streamlines: any gridblock traversed by a streamline attached to a particular well will be tagged as belonging to that well—be it an injector or a producer. For the first time then, SL’s make it possible to divide the reservoir into dynamically defined drainage/irrigation zones attached to individual wells. Properties normally associated with reservoir volumes can now be expressed on a per-well basis, such as oil in place, water in place, pore volume, and even average permeability and porosity. Such data has not previously been available to the practicing reservoir engineer and so there is little in the literature as to how to exploit it. However, one immediate use is apparent: determining displacement and production efficiency for individual wells. This topic is covered in more detail in a separate section, and is one of the reasons for the keen interest currently existing in the technology.

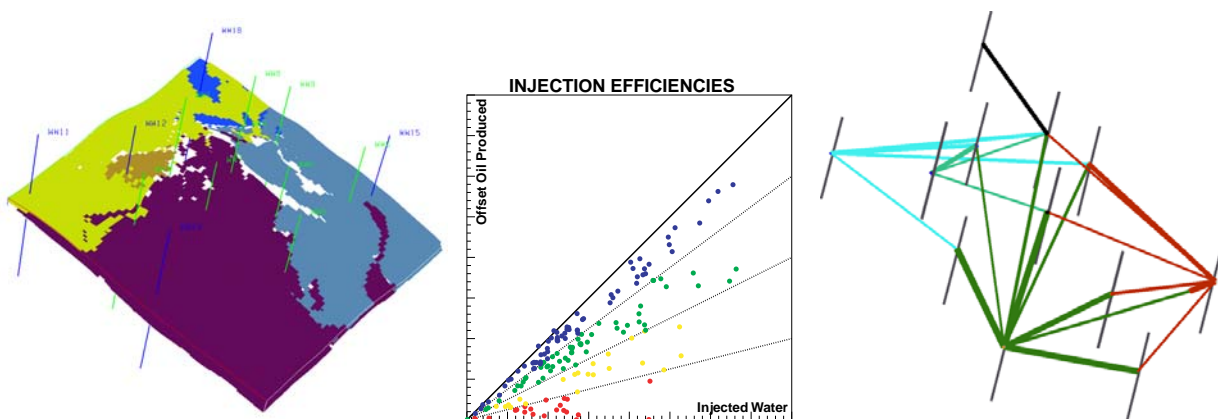


Figure 20: Streamlines produce data not available from more traditional FD approaches such as reservoir volumes associated with individual wells (left), well allocation data between well pairs to calculated injection efficiencies (center), and reservoir connectivity between injector/producer pairs (right). All these combine to a powerful new view of the dynamic behavior of the reservoir.

APPLICATIONS OF STREAMLINE SIMULATION

Streamline simulation has made significant progress over the last 10 years and while the industry is still investigating and exploring the best use of this technology some key applications are clearly emerging. These include waterflood optimization, history matching, quantifying uncertainty in forecasting reservoir performance, and upscaling. More recently streamlines have been used for improved gridding (Mlacnik *et al.* 2004).

Waterflood Optimization

In many ways, the use of SL's for (water)flood optimization is a return to its roots. The improvements in the technology allowing SL's to be used in complex, 3D geological models and with generic well controls opens up an entire new frontier for the application to real systems. The starting point for using SL's in flood optimization is the concept on an injection efficiency, which can be defined as:

$$I_{eff} = \frac{\text{off-set oil production [rb/day]}}{\text{water injection [rb/day]}} \quad (12.)$$

Note the following about the above equation:

- There is an injection efficiency for each active injector in the field. The water injection rate is known (denominator), but the offset oil production (numerator) must be calculated using the information from the well allocation factors (WAF's), which in turn are calculated from the streamlines.
- It is possible to define an injection efficiency on an individual producer/injector pair. In this case, both water injection and offset oil production are computed from the streamlines.
- The injection efficiency in Eq.12. is a ratio of rates and therefore represents an instantaneous efficiency. However, the equation also applies to cumulative volumes, in which case the result would be an average efficiency over a period of time, and is a more accurate calculation of the classical surveillance plot—oil production vs. water injected on per pattern basis.

Although this discussion focuses exclusively on water injection and oil production, the definition of an efficiency can be extended to any type of injected and produced volumes by simply using the appropriate volumes in Eq.12.. A simple pictorial illustration of injection efficiency is given in Figure 21.

This is a simple 100x100x1 heterogeneous grid with wells arranged in the classic five-spot pattern, but where flow is clearly unbalanced. What then is the instantaneous injection efficiency of injector I5? From the streamlines, I5 is connected to four producers: P3, P4, P5, and P7, and the injection rate of I5 is known. However, what is the offset oil production at the producers due to the injection of I5? Pictorially, this is simply the oil produced by the various streamlines bundles that start in I5 and end in the various producers, i.e. the oil produced by the red, green, orange, and yellow streamlines. This data is easily tabulated as part of any streamline simulation and is referred to as well allocation factors (WAF). The same information can also be represented schematically using a Flux Pattern Map (*studioSL 2005*). A flux pattern map shows the connection between well pairs, and the thickness of the lines connecting the wells can be used to represent the strength of the flux between the pairs. Figure 21 shows that 48.5% of the injected volume is directed towards

producer P5, whereas only 14.1% supports P7. The off-pattern producer P4 receives 16.7 of the injected volume of I5.

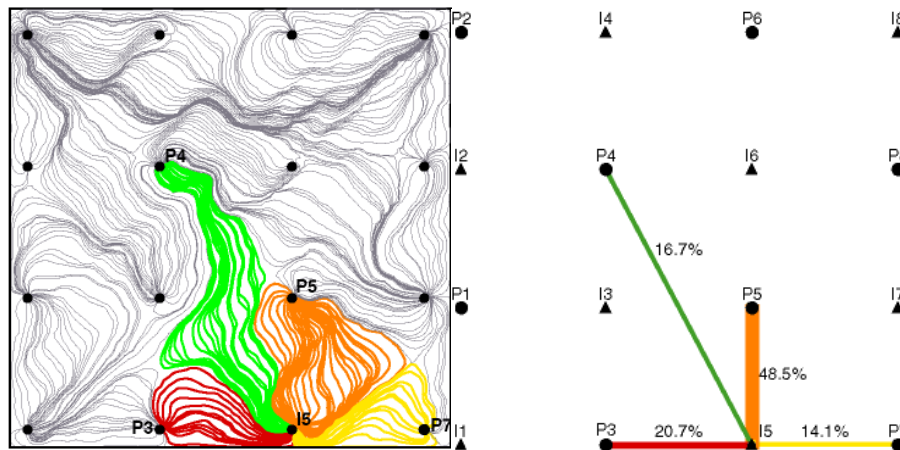


Figure 21: (Left) The injection efficiency of injector I5 is simply the oil produced at the offset producers divided by the injection rate of I5, where the production from the offset producers is simply the sum of the oil produced by the red, green, orange, and yellow streamline bundles. (Right) A Flux Pattern Map (FPmap) schematically depicts the data provided by streamlines, such as the injector-producer pairs and the strength of the connection. This figure shows the FPmap for injector I5 and its offset producers P3, P4, P5, and P7

The goal of any (water) flooding management scheme is to maximize oil recovery for every barrel of volume injected while honoring production/injection constraints, such as total available water, maximum injection/production rates, etc.

From a flood management perspective, there are two approaches that the efficiency data can be used for. Either (a) oil production is maintained utilizing less water, or (b) oil production is increased by better utilization of the available water. Both goals can be achieved with aid of injection efficiencies. The first step in the workflow is to determine the injection efficiencies for each well, and to determine the average injection efficiency of the field. Injection efficiencies can be plotted in many ways and can be color-coded for additional clarification. The most effective way to present well efficiencies is using a scatter plot as shown in Figure 22.

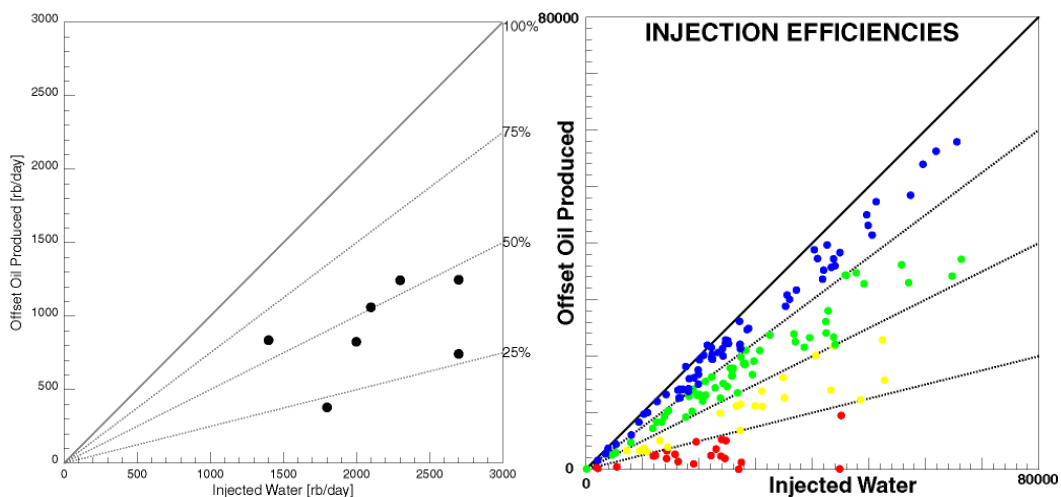


Figure 22: (Left) Injection efficiencies for a reservoir with 7 injectors injecting at 15,000 rb/day and 9 producers producing at 13,500 rb/day. There is a supporting aquifer on the western flank. The average field efficiency is 42.3%. (Right) Injection efficiencies for a Middle Eastern field, color coded for additional clarity.

The dashed lines separate efficiency zones by increments of 25% and the unit slope line represents the limiting 100% efficiency line, i.e. the case in which every reservoir barrel of water injected produces a reservoir barrel of oil at the offset wells. With the individual injection well and field efficiencies determined, the central idea is to re-allocate water volumes by reducing water injection in low efficiency wells and increasing injection in high efficiency wells. “High” and “low” in this context are understood to be in relation to the average field efficiency. One possible reallocation scheme centers on the average field efficiency and smoothly increases or decreases rates depending on where they are compared to the average field efficiency (Thiele & Batycky 2003).

$$\begin{aligned}
 e_i > \bar{e} : \quad w_i &= \text{MIN} \left(w_{\text{max}}, w_{\text{max}} \left(\frac{e_i - \bar{e}}{e_{\text{max}} - \bar{e}} \right)^\alpha \right) \\
 e_i < \bar{e} : \quad w_i &= \text{MAX} \left(w_{\text{min}}, w_{\text{min}} \left(\frac{\bar{e} - e_i}{\bar{e} - e_{\text{min}}} \right)^\alpha \right)
 \end{aligned}
 \tag{13.}$$

where,

e_i is injection efficiency for well i ;

\bar{e} is the average field injection efficiency;

w_{max} is the maximum weight at e_{max} ;

w_{min} is the minimum weight at e_{min} ;

e_{max} is the upper injection efficiency limit;

e_{min} is the lower injection efficiency limit;

a exponent.

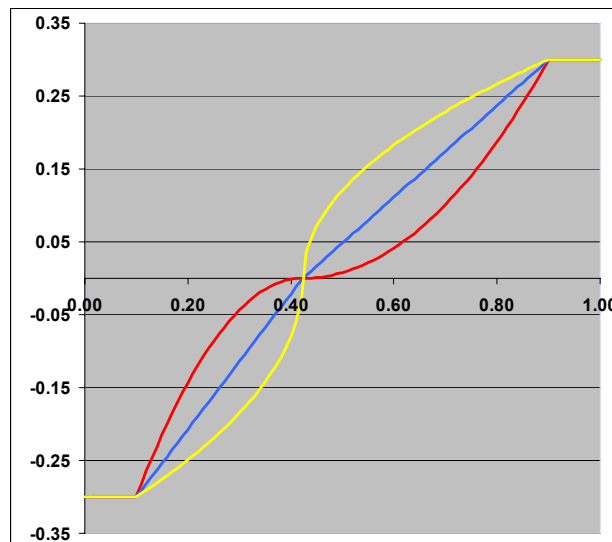


Figure 23: Weights as a function of well efficiencies and exponent α . Maximum and minimum weights are set to 0.3 and -0.3 respectively. Maximum and minimum efficiencies to 0.9 and 0.1 respectively. The exponent is set to 0.5 (yellow), 1.0 (blue), and 2.0 (red). The weights are centered on an average field efficiencies of 42.3%

The new injection rate target rate for a well is then simply determined using

$$q_{new} = q_{old}(1 + w_i) \tag{14.}$$

where w_i is the weight calculated from Eq.(13.).

An Example Application

Reservoir 1 is a 80x81x20 cell reservoir with 9 producers and 8 injectors that are all on a constant total reservoir rate for 1000 days. Total production is 13,500 rb/d and total water injection is 15,000 rb/d. The eastern portion of the reservoir is connected to an aquifer. All the relevant data for the reservoir at 1000 days are depicted in Figure 24.

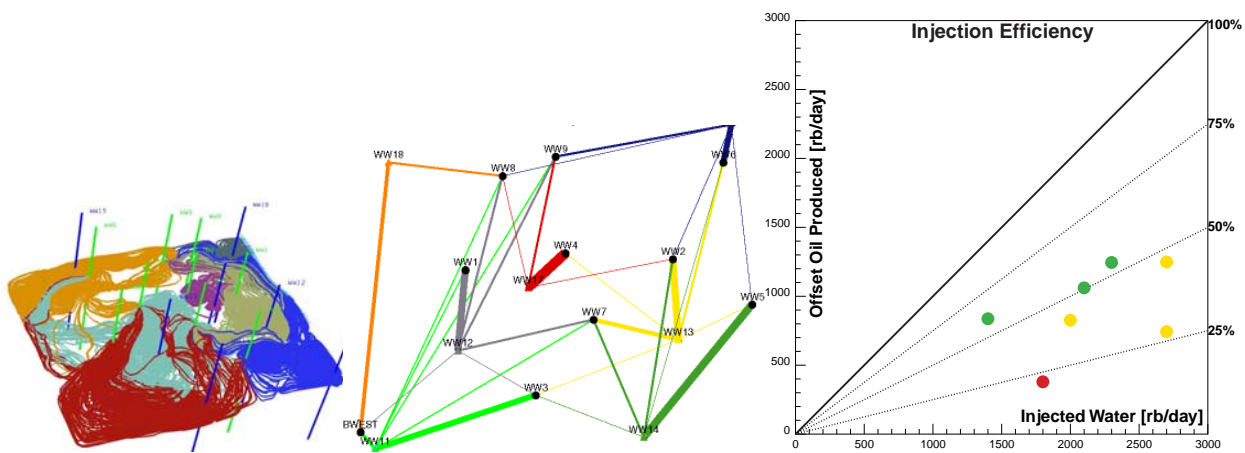


Figure 24: Streamline, FPmap, injection efficiencies at 1000 days for Reservoir 1.

Name	Inj. Wat.	Offset Oil Prod.	%Eff.
WW15	0.2000E+04	0.8259E+03	41.29
WW14	0.2100E+04	0.1061E+04	50.55
WW17	0.2700E+04	0.7434E+03	27.53
WW13	0.2700E+04	0.1248E+04	46.23
WW18	0.1800E+04	0.3791E+03	21.06
WW12	0.2300E+04	0.1245E+04	54.13
WW11	0.1400E+04	0.8364E+03	59.75
FIELD	0.1500E+05	0.6339E+04	42.26

Table 1: Injection efficiency numbers associated with Figure 24.

The rates and associated efficiencies for individual wells are given in Table 1. To implement an injection strategy for Reservoir 1, injection rates are updated every 6 months going forward for a total of 5 years. The field production response is given in Figure 25. The solid lines represent the un-optimized runs (do nothing scenario) whereas the dashed lines are the optimized solution.

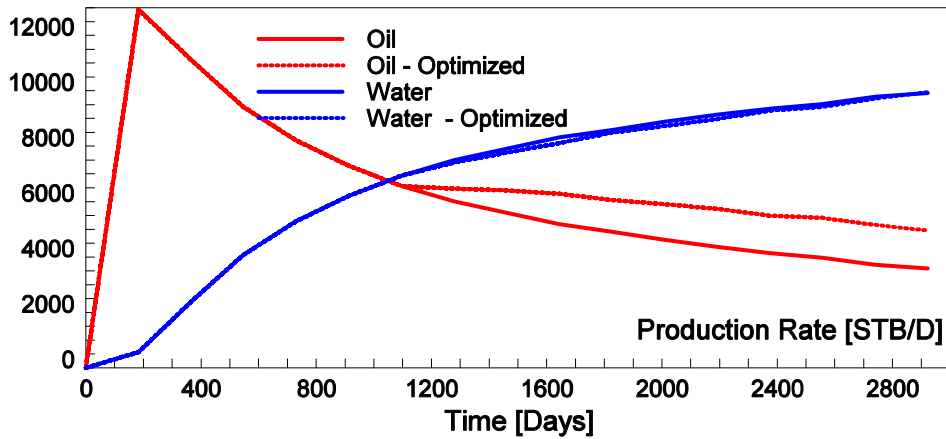


Figure 25: Production rates for the un-optimized solution (solid lines) and the optimized forecast (dashed lines). Incremental oil recovery of the optimized injection schedule is of 2.17MM STB over 5 years, and a decrease in water production of 0.26MM STB. Total field injection is a constant 15,000 rb/day over the life of the field.

Changing Injection/Production Rates

It is important to understand that as the injection rates are changed, the offset production rates of the impacted producers must be changed as well, otherwise the geometries of the streamlines is significantly altered. Thus, an increased injection rate must be accompanied with an exact offset increase in production rates. By how much to increase offset production can be calculate using the WAF's. Consider Figure 26, which shows the SL's and the corresponding FPmap for WW13.

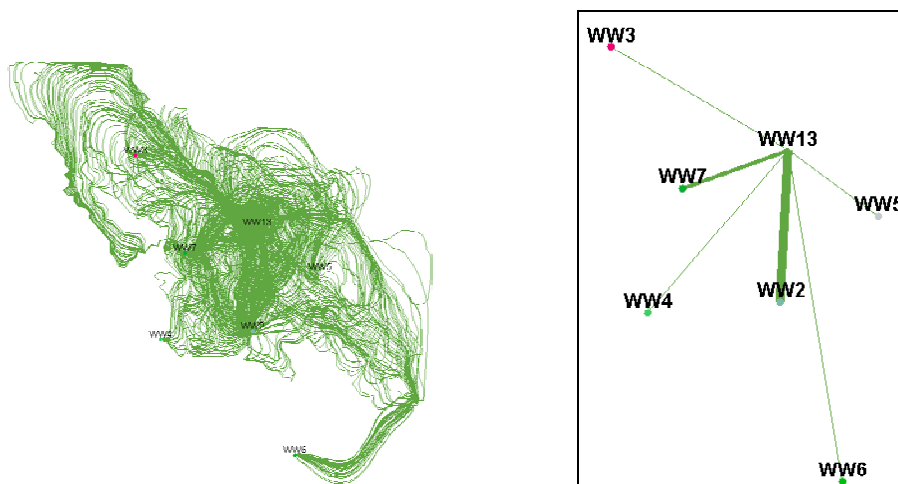


Figure 26: Streamlines and corresponding FPmap for injection well WW13.

The rates and injection efficiencies for each branch of the FPmap are given in Table 2.

WW13	WW2	WW3	WW4	WW5	WW6	WW7
Wat in	1686	23	74	109	98	709
Oil out	896	22	67	51	25	264
%Eff	53.1%	92.4%	89.8%	46.5%	25.4%	37.3%

Table 2: Data used to calculate the PIE’s for each branch of the FPmap in Figure 26.

The total injection rate for well WW13 is changed by taking the injected volume associated with each branch (water in), increasing/decreasing it according to the efficiency of that branch, and then summing all the new injection volumes of each branch. Thus,

$$q_{WW13} = \sum_i q_i(1 + w_i) \tag{15.}$$

Since the target rates for the injectors we determined by increasing/decreasing the total reservoir rate of each connection in the FPmap, then each producer can be increased/decreased by exactly the same amount on the other end. In other words, the production target rates for each producer are simply determined by adding the individual rate increase/decrease already calculated on the injection side. The FPmap colored by producers is shown in Figure 27(left). Consider the producer WW7 (Figure 27 right), which is connected to the 5 injectors WW11, WW12, WW13, WW14, and WW17. Since rate increases/decreases for each of these connections have already been calculated, the production rate targets are simply a summation of calculations already done for the injectors.

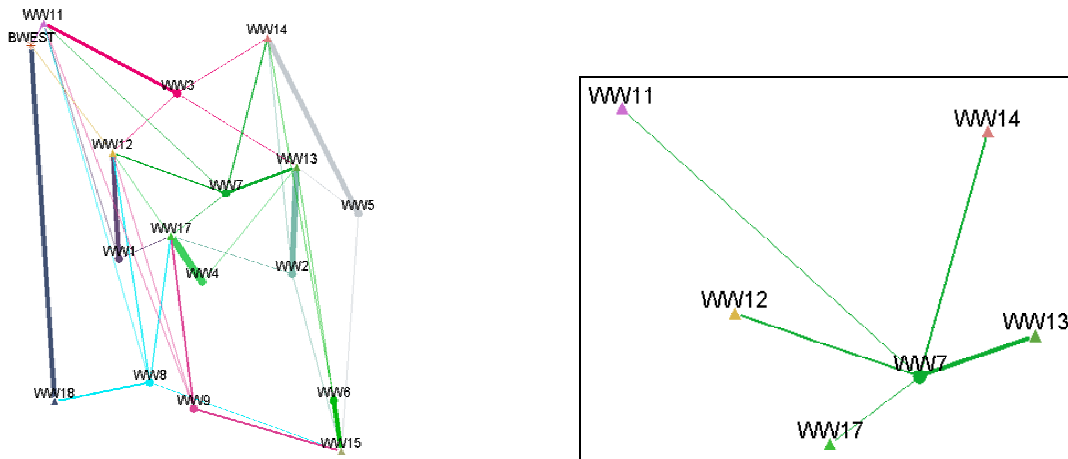


Figure 27: (left) FPmap colored by producers. (right) FPmap for WW7. The production target rate for WW7 is simply calculated by adding/subtracting the Δq ’s already calculated for each of the 5 connections to the various injectors.

Rates changed to the injection wells beyond 1000 days compared to the un-optimized case are shown in Figure 28. Notice how WW11, WW14, WW15 see the injection rate increased vs. WW13, WW17, and WW18 that see a significant reduction in injection. WW12 is already near its optimal rate and sees little change. Four production wells seem to be significantly affected by the

optimization: WW3 and WW9 see a significant increase in oil production whereas WW4 and WW6 are able to maintain oil production with a significantly smaller water production. Thus the summary plot (Figure 25) can be explained by the fact that WW3 and WW9 now produced significantly more oil and water, while WW4 and WW6 produced significantly less water—thus the net field effect is a significant increase in oil production while maintaining water production at pre-optimized levels.

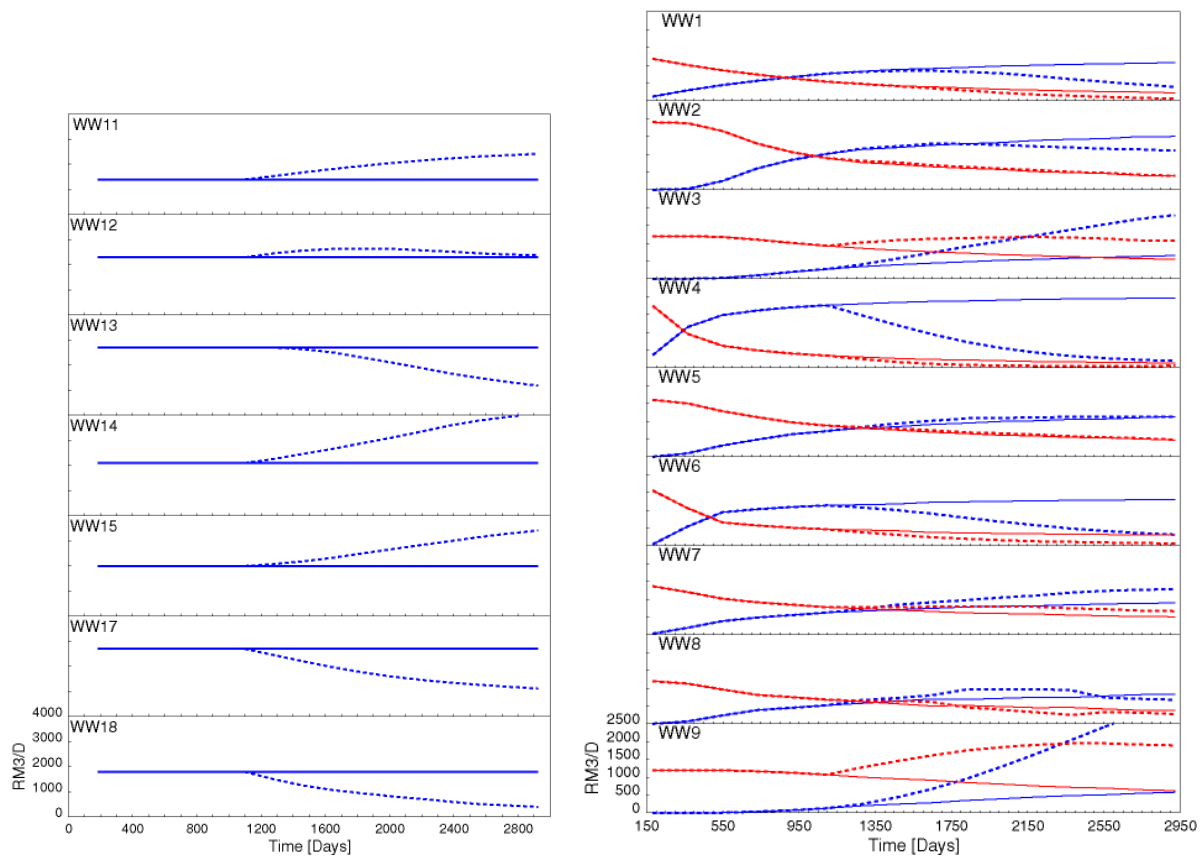


Figure 28: (Left) Rates changes for injection wells beyond 1000 days resulting for the optimized forecast (dashed lines) compared to the un-optimized case (solid lines). All plots have a y-scale of 0-4000 STB/D. (Right) Rate changes for production wells. Optimized cases are dashed lines, un-optimized cases are solid lines. All plots have a y-scale of 0-2500 STB/D.

Treatment of Aquifer

Loss of injection volumes to open boundaries of the reservoir (aquifers) or possible production due to aquifer support must be treated separately since the strength of the aquifer cannot be controlled. To reduce the loss of injected volume to a connected aquifer (i.e. inefficient use of water), the algorithm simply reduces the injection rate of the particular injector(s) that are losing volume by a preset percentage without changing any offset production rates. For the example used here, the reduction in rate due to loss of water to open boundaries/aquifers was set to be 25%. As the optimization is repeated at preset time intervals, the loss of injected volume can be significantly reduced over the forecast period. Production due to aquifer support, on the other hand, remains unaltered and left as is.

The workflow used in this example is shown in Figure 29. For a true optimization approach, the workflow in Figure 29 should be iterated on using an objective function to ensure either minimum

water use over the forecasted period or/and maximum oil production. This because the problem is inherently nonlinear: as the rates are changed the SL's change as well.

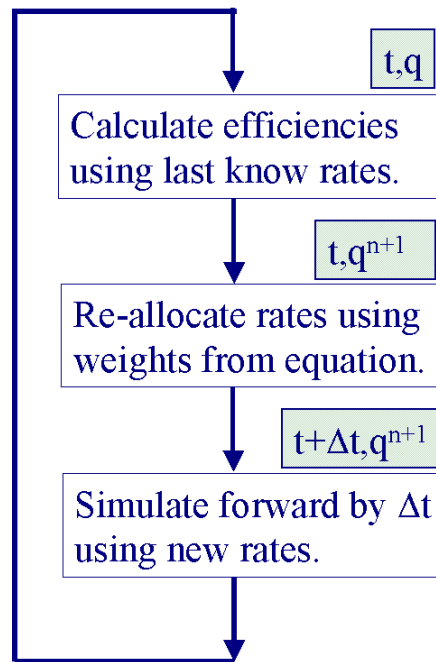
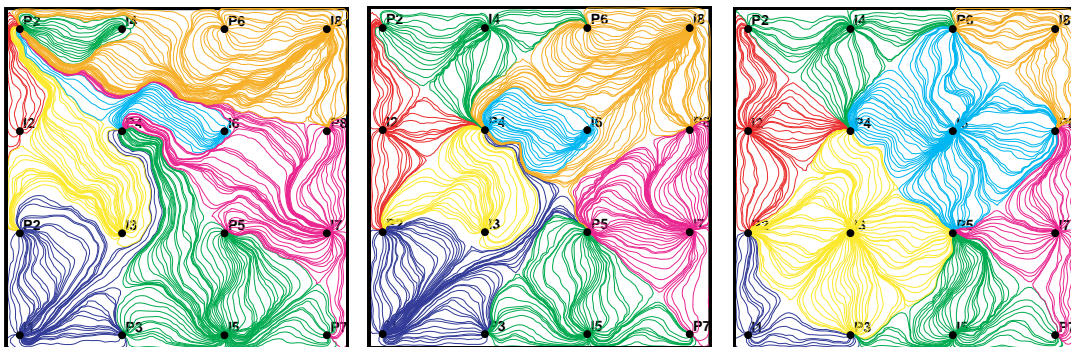


Figure 29: Workflow used for water management of reservoir 1.

Pattern Balancing

Closely related to flood optimization is the ability of streamlines to aid in balancing patterns. By using the WAF's, the amount of injected fluid supporting any producer in the field is known, and therefore the allocation of fluid between injectors and producers in a pattern is obtained as part of any flow simulation. This also means that streamlines can immediately point out any fluid loss to wells outside a pattern—a potentially serious problem—and something empirical methodologies simply cannot capture. Figure 30 show a simple re-balancing of rates illustrated using information of streamlines and FPmaps. Rates are progressively changed so as to get a more even distribution of streamlines associated with injectors (irrigation volumes) or producers (drainage volumes).



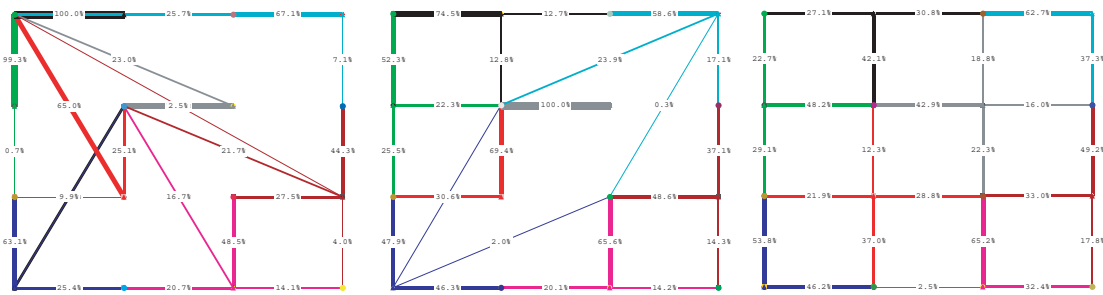


Figure 30: Knowing the allocation of flow between wells and the visual display of streamlines allows patterns to be balanced more correctly and efficiently than with current techniques. From left to right: rates are progressively changed to yield a balanced pattern.

History Matching

Another particularly promising application of SL simulation is in the area of history matching. Streamlines are easily associated with individual wells and delineate volumes of the reservoir associated with those well, and should therefore be useful in the tedious model calibration exercise reservoir engineers must go through—generally referred to as history matching (HM)—before doing any production planning and forecasting.

In addition to opening a new avenue for pursuing the HM problem itself, having an efficient and fast method to generate reservoir responses is an advantage even in the context of more traditional HM techniques. Faster forward simulations lead to shorter turn-around times between model changes, and the ability to simulate models with more gridblocks between wells is known to lead to more reliable predictions.

There have been three main approaches to using SL's for history matching in the past:

1. Defining average reservoir regions associated with wells and then changing grid properties directly in these regions to match production response (*Emanuel and Milliken 1997,1998*);
2. Derivation of analytical sensitivity coefficients which are then used to set-up an inverse problem (*Wen et al. 1998, Vasco et al. 1999*);
3. Modify grid properties traversed by streamlines to reduce/increase breakthrough times along these streamlines (*Wang and Kovsky 2000; Caers et al. 2002, Agarwal and Blunt, 2001,2004*).

All three methods have shown to be useful in wide a variety of settings under different operating conditions. The AHM approach of Emanuel and Milliken (*1997,1998*) has been applied with success on a number of real fields. Its most distinguishing feature is that it does not rely on any mathematical algorithm to attempt convergence, and instead forces the engineer to use judgment and experience to modify the underlying geological model parameters. In the usual manner, the updated model is re-run and checked against field performance. The process is continued until an acceptable match is achieved. Deriving analytical sensitivity coefficient from streamlines is also a particularly efficient approach, but on the downside relies on fixed streamline paths and faces the solution of an inverse problem once the sensitivity coefficients have been determined. If the initial problem is large, the solution of the inverse problem might be more computationally intensive than the forward simulation with the streamlines. Few, real field cases have been HM'ed using this method. Several authors (*Wang and Kovsky 2000; Agarwal and Blunt, 2001,2004*) have presented direct modification of gridblock properties associated with individual streamlines. However, the final geological model might not honor prior geological information. In the case in which the

initial mismatch is significant, the final geological model is likely to deviate significantly from the prior geological continuity model.

A promising approach has recently emerged in the context of geostatistical methods for history matching under geological control (Caers *et al.* 2002, Caers 2003, Le Ravalec-Dupin and Fenwick 2002, Gross *et al.* 2004, Caers 2005). The main idea is to use the ability of SL to divide the reservoir into zones associated with wells (see Figure 31).

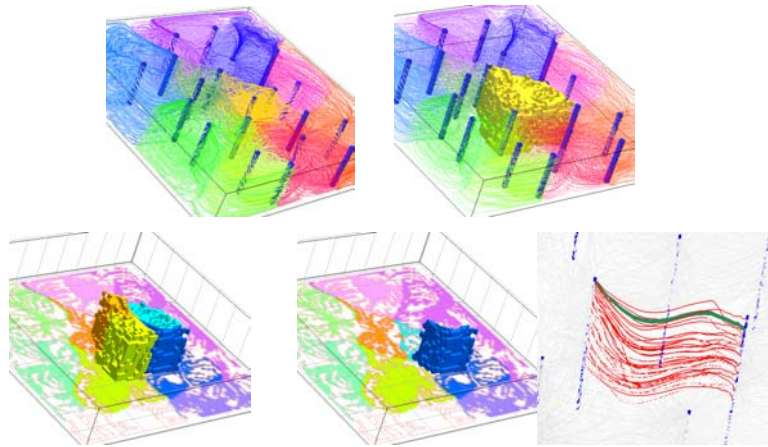


Figure 31: At any particular time (set of streamlines), it is possible to associate volumes of the reservoir (grid blocks) with individual wells. There are three scales of interest SL are able to define: (a) the volume associated with a drainage/irrigation zone of a well; (b) the volume associated with a well-pair; and (c) volume associated with an individual streamline (courtesy H.Gross).

Perturbations can be applied to all three scales with the overarching constraint being that the prior geological continuity model is honored at all times. As a result, the perturbations are not applied directly to the underlying grid, but rather to the parameterization of the geological continuity model. The final, HM model will therefore belong to the set of all possible realization that can be generated from the assumed prior geological scenario. There are two significant implications that follow from this approach:

1. If the prior geological scenario described through the parameterization is wrong, there is nothing in the HM process that will correct this. In other words, the HM approach will not be able to generate an alternate geological scenario—it can only hope to find an acceptable geological realization from the infinite set of realization that can be build for a particular scenario.
2. At any stage in the HM process, the geological model will be consistent and geologically realistic. It is assumed, that this greatly improves the reliability of the model for forecasting purposes.

What can happen when local changes are mapped directly onto the underlying grid can be seen in the rather extreme example shown in Figure 32. Changing permeability directly along the streamline paths results in an unrealistic permeability distribution (Figure 32-Left) that has little resemblance with the original geology, although the history match is perfectly acceptable (not shown here). Feeding the changes back into the parameterization of the original geological algorithm, on the other hand, produces the image (Figure 32-Right) consistent with the original geological continuity model and with an equally good production match. What favors the right

image, of course, is that conforms to the geologists model of what the reservoir could look like. There is no reservoir that looks like Figure 32-Left.

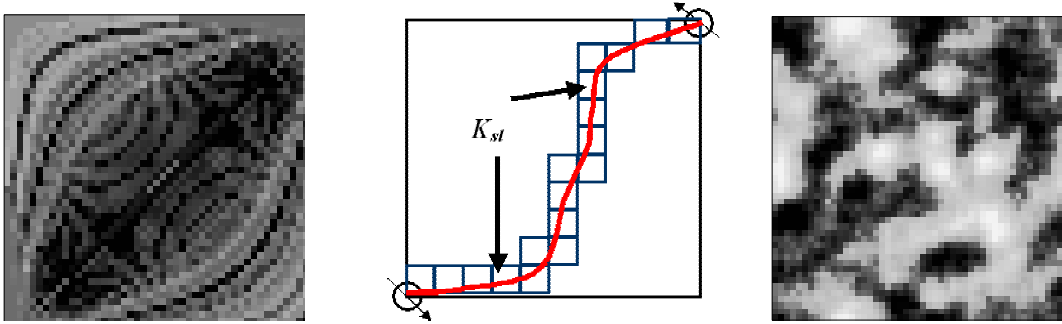


Figure 32: (Left) Mapping permeability changes from streamlines directly to the underlying grid causes inconsistent images of the geological model. (Right) Feeding the changes into the parameterization used to create the geological models in the first place allows creating images that are geologically consistent and match production history (courtesy of J.Caers).

The perturbations to the parameters of the geological continuity model can come from many sources, including “experience-based” multipliers of reservoir regions. But SL’s have two distinct advantages: (1) the mismatch between production data and simulation can be related back to permeability and porosity via TOF and (2) streamlines are able to delineate volume of the reservoir to which changes should be applied. A discussion of these two key ideas follows next.

The time-of-flight is the time it takes a neutral particle to travel along a streamline. Because the streamline are an instantaneous picture of the velocity field, how quickly or how slowly a particle travels is a function of the underlying velocity field and therefore of permeability and porosity. Using the definition of TOF, it is simple to show the TOF along a streamline is proportional to permeability and inversely proportional to porosity:

$$\tau = \int \frac{\phi}{|\vec{v}_t|} d\xi \quad \rightarrow \quad \tau \propto \frac{\phi}{k}. \quad (16.)$$

Consider now a generic mismatch between historical and simulated water production for a particular producer as shown in Figure 33. For now, assume the following: (a) water moves along each streamline in a piston-like fashion and (b) assume the streamlines are fixed in the simulation model for the time period over which the mismatch is measured. Clearly, the desire is to shift the simulation curve by an amount Δt such that the mismatch between historical and simulated water production is minimized. In other words, streamlines that are breaking through too late must see a reduction in their TOF. It is thus possible to write a ratio of time flights and an updated porosity/permeability ratio as

$$\frac{\tau^{new}}{\tau^{old}} = \frac{\left\langle \frac{\phi}{k} \right\rangle^{new}}{\left\langle \frac{\phi}{k} \right\rangle^{old}} \quad \rightarrow \quad \left\langle \frac{\phi}{k} \right\rangle^{new} = \frac{\tau^{old} + \Delta\tau}{\tau^{old}} \left\langle \frac{\phi}{k} \right\rangle^{old} \quad (17.)$$

where the average porosity/permeability ratio is calculated as a resistance in series expression along a streamline as follows

$$\left\langle \frac{\phi}{k} \right\rangle = \frac{1}{\tau} \sum \Delta \tau_i \left(\frac{\phi}{k} \right)_i \quad (18.)$$

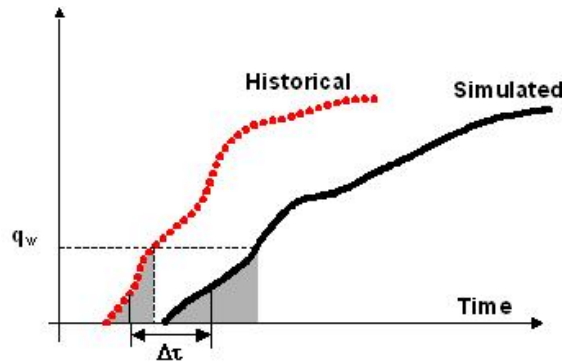


Figure 33: The time-mismatch between historical production data and simulated data allows to define a TOF-correction that can be applied to individual streamlines as per Eq.(17.).17.

Thus, if the simulation curve needs to be shifted to better match historical production data, the shift requires increasing/decreasing the average porosity/permeability ratio along the streamlines by a ratio of TOF's. Equation (17.) is straightforward. However, it is not immediately obvious how the new porosity/permeability ratio is to be propagated back to the underlying grid. A direct mapping to the grid is not an acceptable solution since it leads to pictures such as the one shown in Figure 32-Left.

One approach (Gross *et al.* 2004), is to make use of the ability of the streamlines to define volumes associated with particular wells and derive the average directly from that region. Using that approach one might write that

$$\left\langle \frac{\phi}{k} \right\rangle^{old} \approx \left\langle \frac{\phi}{k} \right\rangle_{vol \text{ defined by streamlines}} \quad (19.)$$

where the average itself might be calculated using an arithmetic, harmonic, or geometric average. The old porosity/permeability ratio could also be the local varying mean (LVM) used in the geostatistical algorithm when generating the realization in the first place. The new permeability-porosity ratio is then calculated using the ratio of TOF's (Eq. 17.) and propagated back to the geological model via an updated local varying mean (LVM) or through block kriging (BK). There remain, however, some loose ends: Eq's. 17. and 19. say nothing about which directional permeability to use. Most models are populated with an areal permeability ($k_{areal}=k_x=k_y$) and a vertical permeability (k_z). Also, which volumes (Figure 31) associated with a producer should be used for propagating the average back through the geostatistical algorithms? The entire drainage volume of a producer, the volume associated with an injector-producer pair, or the individual streamline scale? And finally, SL's change over time, so a producing well will have multiple LVM regions that need to be enforced simultaneously. These are areas that are currently being actively researched.

A different approach to determining the average permeability and propagating the correction back is that of Le Ravalec-Dupin and Fenwick (2002) and Caers (2003). In their work the Dykstra-Parson analogy of Wang and Kovscek (2000) is used. The average permeability-porosity ratio along a streamline is a TOF-weighted harmonic average (resistance in series) of the grid block values a streamline encounter as it goes from injector to producer, and the average of a bundle of streamlines is a flux weighted arithmetic average (resistance in parallel):

$$\begin{aligned} \left\langle \frac{\phi}{k} \right\rangle^{sl} &= \frac{1}{\tau_{sl}} \sum_{i=1}^{N_b} \Delta \tau_i \left(\frac{\phi}{k} \right)_i \\ \left\langle \frac{\phi}{k} \right\rangle^{bundle} &= \frac{\sum_{sl=1}^{Nsl} q_{sl}}{\sum_{sl=1}^{Nsl} q_{sl} / \left\langle \frac{\phi}{k} \right\rangle^{sl}} \end{aligned} \quad (20.)$$

Even in this formulation the problem of which block directional permeability to use in calculating the average streamline permeability-porosity ratio persists. Le Ravalec-Dupin and Fenwick (2002) and Caers (2003) then propose an optimization technique (gradual deformation/probability perturbation) to update the geological model. The geological realization is deformed gradually into a new realization such that the new model yields average values of the porosity/permeability ratio—either on along individual streamline or for a bundle—that minimize an objective function. A new streamline simulation is then run on the gradually deformed permeability field leading to new streamlines and the process is repeated until a global minimum in the objective function is reached.

Ranking & Uncertainty in Reservoir Performance

When streamlines re-appeared in the early nineties, the profound impact geological models could have on the quality of simulation results was generally understood. The proliferation of sophisticated algorithms to model structure, faults, and properties is a testament to that. One of the earliest applications perfectly tailored for low-physics, high-speed, SL simulations seemed to be the ranking of fine-scale geological models—models that were clearly too large for traditional approaches but which needed ranking beyond the usual static variables such as hydrocarbon pore volume or connected volumes. Yet, ranking has been slow to emerge as one of the key applications of SL simulation. Why?

As pointed out by Gilman et al. (2002) the analysis for ranking and assessing uncertainty is not as straightforward as simply simulating a number of equiprobable geological models. Complicating matters, uncertainty in future recovery can be as much a function of flow physics, well patterns, and well rates as it can be due to static geological variability. Thus, the geoscientist must straddle with confidence two distinct disciplines—geomodeling and reservoir engineering—to perform a proper analysis of uncertainty. Adding an economic component only complicated things further.

The dependence of rank on flow physics has been demonstrated via a very simple 3D, quarter-five spot example by Thiele and Batycky (2001). Figure 34 shows 30 equiprobable realizations in which the rank determined by TOF—linear, single phase flow where the TOF of the fastest streamline is taken as a cutoff for all other streamlines and the swept pore for that TOF's is used to rank the models—versus the recovery at breakthrough with increasing complexity of displacement physics. Figure 34 shows how quickly the ranking can change as flow physics is added to the simulation. Picking a P₁₀, P₅₀, and P₉₀ based on TOF ranking is not a good indicator of how recovery for more complex displacement physics might behave. In other words, steady-state, single-phase flow might not always be a good proxy for engineering more complicated enhanced or improved recovery

mechanisms in a field. Adding geological variability to the mix of variable only adds the complexity of the problem. An efficient simulation approach alone—like SL simulation—is simply not sufficient to allow quantitatively useful analysis of uncertainty in reservoir performance. A statistical framework is needed that can channel the information into answers sought by engineers: which parameters contribute to the largest uncertainty? Can the uncertainty be reduced via additional data acquisition? What future reservoir management offers the best risk-return ratio?

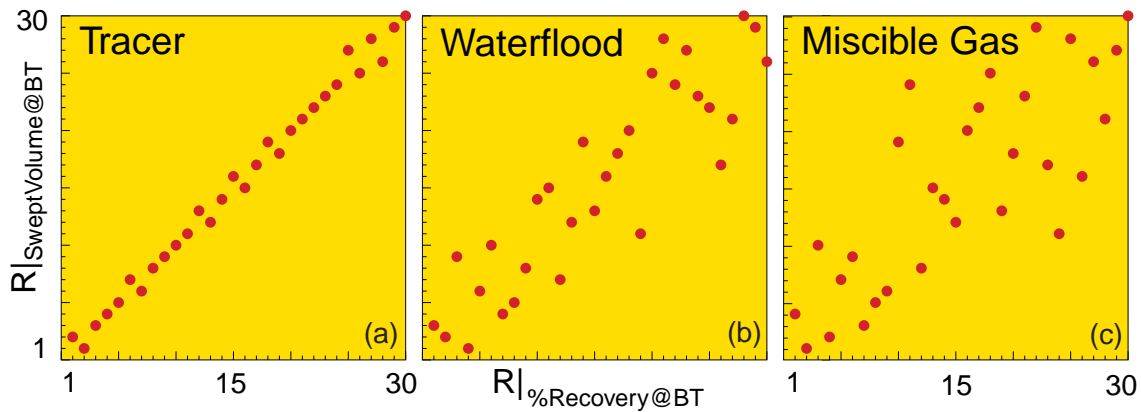


Figure 34: Flow physics can significantly change the ranking behavior of systems of geological models. Here, 30 realizations are cross-plotted using the TOF-rank with the rank obtained using recovery at breakthrough with progressively more physics (from Thiele and Batycky, 2001).

The first difficulty in assessing uncertainty in reservoir performance is sampling the input parameter space. Consider the following simple scenario: a single, large geo-cellular model—maybe having 2-5 million cells—is to be assessed for uncertainty in reservoir performance. Because the model is too large to simulate directly, a number of upscaled models are derived. Considering just three upscaling methods, two sets of relative permeabilities, and five fault models leads to a total of 90 models that would need to be simulated, and the number is easily increased into the 1000's by considering just a few more additional parameters. Clearly, selecting models by a simple random Monte Carlo approach will not be successful if the number of parameters to be investigated is significant. A more intelligent sampling algorithm is required. One such approach has been suggested by Christie et al. (2002) which makes use of the Neighborhood Algorithm (NA), a stochastic sampling algorithm developed for earthquake seismology. The NA works by adaptively sampling the parameter space using geometrical properties of Voronoi cells to bias the sampling to regions of good data fit. The resulting ensemble of models represents a much smaller subset that can be used to predict the uncertainty in future performance using a tractable number of models, all of which are a good fit to past performance. Another alternative to sampling and evaluating the search space is to use evolutionary algorithms (Schulze-Riegert et al. 2002) which are characterized by only requiring the value of the objective function and do not need any gradient information. Evolutionary algorithms are robust and are inherently parallel, though convergence remains an outstanding issue and depends to a large extent to the amount of soft, expert knowledge provided by the user. Experimental design offers yet another approach to span the input parameter space in a systematic way so as to reduce the computational effort (White et al. 2001, Manceau et al. 2001).

Gilman et al. (2002) have pointed out the need for a more comprehensive statistical framework for assessing the impact of geological uncertainty on future performance. Regular well patterns—not necessarily representative of the actual well patterns or injected fluid rates existing in the field—can be used as a basis for ranking future performance. Because uniform patterns cover the entire area of interest, and thus volumes of the reservoir away from known conditioning data, a more representative rank of the connectivity of the reservoir can be determined. In other words, the impact of the geological variability away from existing wells is emphasized here since, it is argued,

that these areas are the ones will have a longer-term effect of performance and affect the decision of potential infill wells and recovery mechanisms.

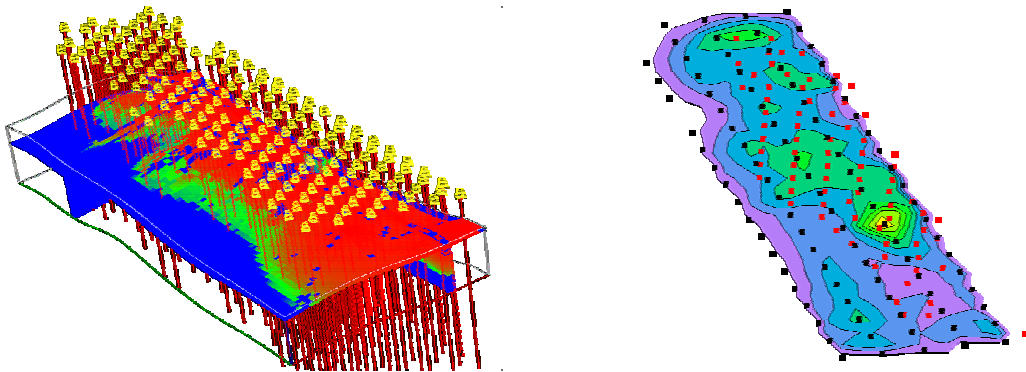


Figure 35: (Left) Using a regular pattern of wells can be used to assess the impact of geological variability away from existing wells and the associated constraining data. (Right) A map of normalized standard deviation in oil recovery for all realizations can be used to show the largest uncertainty in oil recovery. (From Gilman et al. 2001)

Upscaling and Streamlines

Three SL features seem to be particularly useful for upscaling:

1. Producing fine-scale reference solutions (Samier et al., 2002).
2. Derive upscaled grid properties using streamlines (Christie and Clifford, 1997).
3. Lump cells using streamlines (Castellini et al. 2000, Portella and Hewett, 2000).

There are extensive variations on these themes in the literature, which are not repeated here. The reader is encouraged to review the many excellent papers on this topic. In general, contributions can be separated into the application of streamlines as they pertain to validating upscaling methodologies, and application of streamlines as they pertain to actually generating average, upscaled properties.

In the area of validation, recent work by Samier et al. (2002) suggest that streamlines might offer an additional feature beyond simply generating fine-scale reference solutions against which to check upscaled solutions. The premise is that for upscaled system to have similar dynamic behavior as the original fine-scale model, wells should be draining similar volumes and those volumes should be connected in a similar way. Streamlines provide just that information. Comparing connected volumes over time for individual wells would offer a novel way to analyze the relative performance of upscaling algorithms.

Figure 36 and Figure 37 illustrate this idea using an example from Samier et al. (2002). Figure 36 shows that the streamline patterns of the upscaled models reproduce the fine-scale streamlines only in certain parts of the field. Figure 37 quantifies this discrepancy and compares it to the fractional flow behavior of the well. Well P2C is a good example where matching the well pore volume over time also leads to a good match of the water fractional flow. Well P3, on the other hand, has no match of the fine-scale pore volume, but the fractional flow is acceptable. Figure 37 makes another interesting point: upscaling method 1 seems to work well for well P2C where as method 2 does a better job for well P4 and GA. The pore volume for P3 is not reproduced by either method. Thus, different local geological representations might require different upscaling methods—there is no one-method-fits-all solution when it comes to upscaling. SL's might offer a powerful diagnostic in this case.

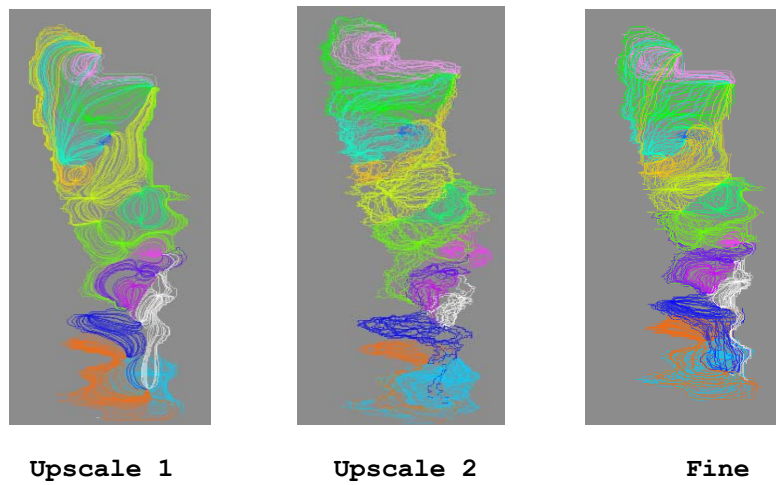


Figure 36: Streamlines colored by producers for two upscaled model and the reference fine-scale model. Good upscaling should produce similar streamlines patterns and volumes associated with individual wells between the fine-scale model and the upscaled models (from Samier et al. 2002).

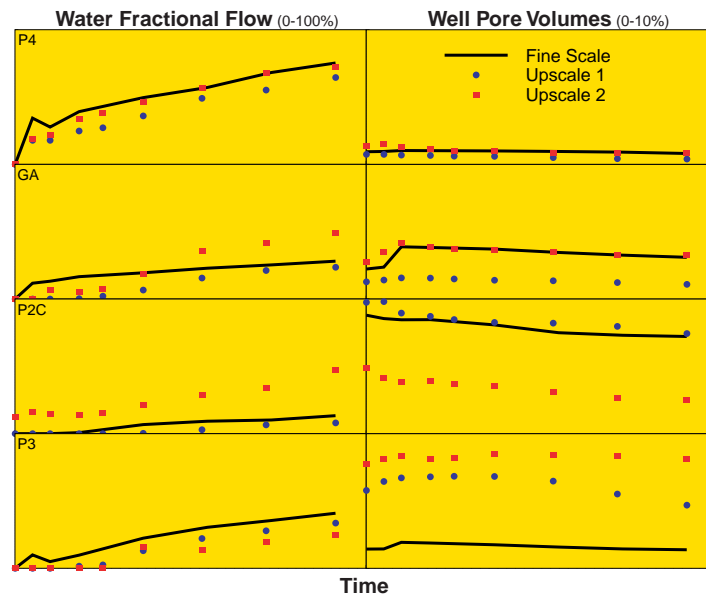


Figure 37: Streamlines allow to compare volume associated with wells between fine-scale and coarse-scale problems. Wells having good agreement on pore volume between fine-scale and coarse scale are likely to give better matches.

An upscaling analysis based on well volumes and geometry might, in the end, be more relevant than simply comparing production profiles. For real field cases, it is well known that upscaling can eliminate smaller faults, transmissibility barriers, and other geometrical features so as to significantly change the flow pattern and drainage volume of a well. In such cases, there is no tweaking of flow parameters (such as relative permeability) that can remedy this problem, though a match with unphysical flow parameters might still be possible. The problem is one of flow geometry, and until the flow patterns in the upscaled model are not adequately matched to what is seen in the fine-scale model it is probably of little use to pursue approaches based on other parameters.

Dual-Porosity Simulation Using Streamlines

A dual porosity formalism for SL simulation has been presented Di Donato et al. (2003, 2004), which was followed by work of Al-Huthali and Datta-Gupta (2004). The key idea in Di Donato et al. is that there is a flowing medium and a non-flowing medium. A streamline always traverses the flowing medium, and interacts with the non-flowing medium through a transfer function. Thus a single porosity (SP) block can either be a “matrix” block or a “fracture” block. Both are treated as a flowing medium along the streamline. Conversely, a dual porosity (DP) block will have a flowing medium (the fracture) represented along the streamline and a non-flowing medium (the matrix) coupled to the streamline via a transfer function. See Figure 38 for a graphic representation of this concept.

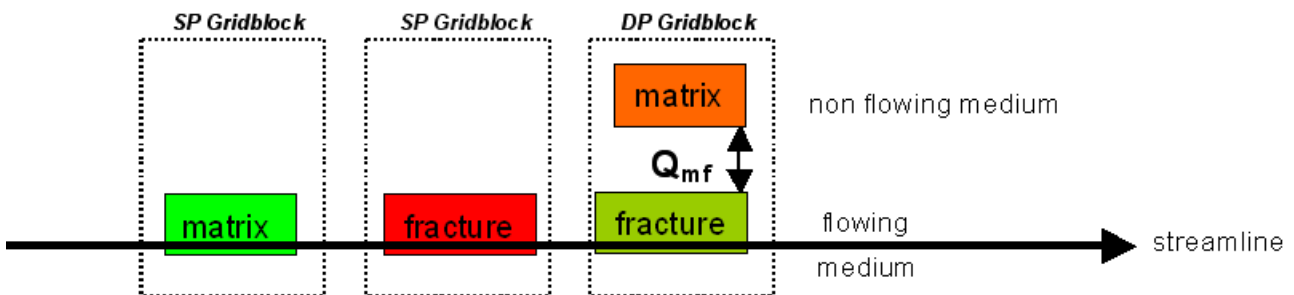


Figure 38: Conceptual drawing of SP and DP gridblocks intersected by a streamline.

Di Donato et al. implemented a linear transfer function, the Kazemi et al. (1992) transfer function, and the capillary pressure driven model found in conventional grid-based simulation methods (Gilman & Kazemi 1983). Transfer between fracture and matrix is assumed to occur only because of an explicit saturation gradient (linear and Kazemi models) or capillary pressure difference (conventional model). Additionally, using the incompressible fluid assumption, the reservoir volume rates of water imbibing into the matrix and oil draining into the fracture are exactly the same but of opposite sign. Thiele et al. (2004) extended the approach of Di Donato et al. (2003,2004) to more realistic geological systems that contain both single and dual porosity cells, as well as heterogeneous porosity and permeabilities distributions for both the matrix and the fractured regions, and multiple relative permeability regions.

Mixed SP/DP systems give rise to a large distribution in cell volumes along a 1D profile for each streamline with relatively small cells potentially forcing the 1D explicit solver into unrealistically small time steps. To solve this problem, Thiele et al. (2004) merged small volume cells with their neighbors as one way to eliminate them a SL’s 1D profile. However, because not all small cells can be merged with their neighbors—for example, SP cells cannot be merged with DP cells—the 1D solver method was modified to be adaptive implicit so that any remaining small cells are treated implicitly. Results showed that binning and implicitness have a large and favorable impact on runtimes with little adverse affect on solution profiles.

A 3D SP/DP Example

Thiele et al. (2004) presented an example constructed by modifying the 60x220x17 SP upscaled SPE10 data set. The upscaled permeabilities were used to construct both a matrix and fracture permeability field, as well as multiple relative permeability regions. Specifically, the matrix and fracture permeabilities were set to 1/10th and 10 times the upscaled permeabilities respectively. Matrix was assumed to be present throughout the entire model but in areas where the fracture permeabilities was <100 mD, fractures were assumed to not be present (SP gridblocks). In total there were 126,000 DP gridblocks and 98,000 SP gridblocks. Relative permeability regions were created as follows: the fracture system represented one rock region (straight line fractional flows),

matrix blocks in the DP region were divided into 3 regions based on permeability cutoffs, and SP gridblocks were given their own relative permeability curves. As the SL method does not include capillary pressure in the flowing medium transport equations, care was taken to remove capillary pressure from the fracture and the SP matrix relative permeability curves for validation with a standard finite difference model. As in the original SPE10 problem, an injector was located in the center of the model, while a producer was located at each corner. Where a well's path intersected DP gridblocks it was completed in the fracture medium of a DP gridblock, otherwise it was completed in the matrix of SP gridblocks. Producers were on total liquid rate control with rates set such that producers in higher permeability regions had a higher liquid rate compared with those in lower permeability regions. The injector was on pressure control. The volume replacement ratio (VRR) was exactly one.

Figure 39 is a comparison of oil rates for each producer for the SL and finite difference solution. Although the oil production trends are similar for producer 4, SL simulation predicts earlier water breakthrough. As shown in Figure 39 water breakthrough is earlier because SL's shows a sharper thinner water front in the fracture system than finite differences for the layer where breakthrough to producer 4 first occurs. This is typical of highly heterogeneous models where streamlines do a good job of capturing high permeability streaks. The remaining well profiles agree better because there are less continuous streaky high perm zones between the injector and these wells.

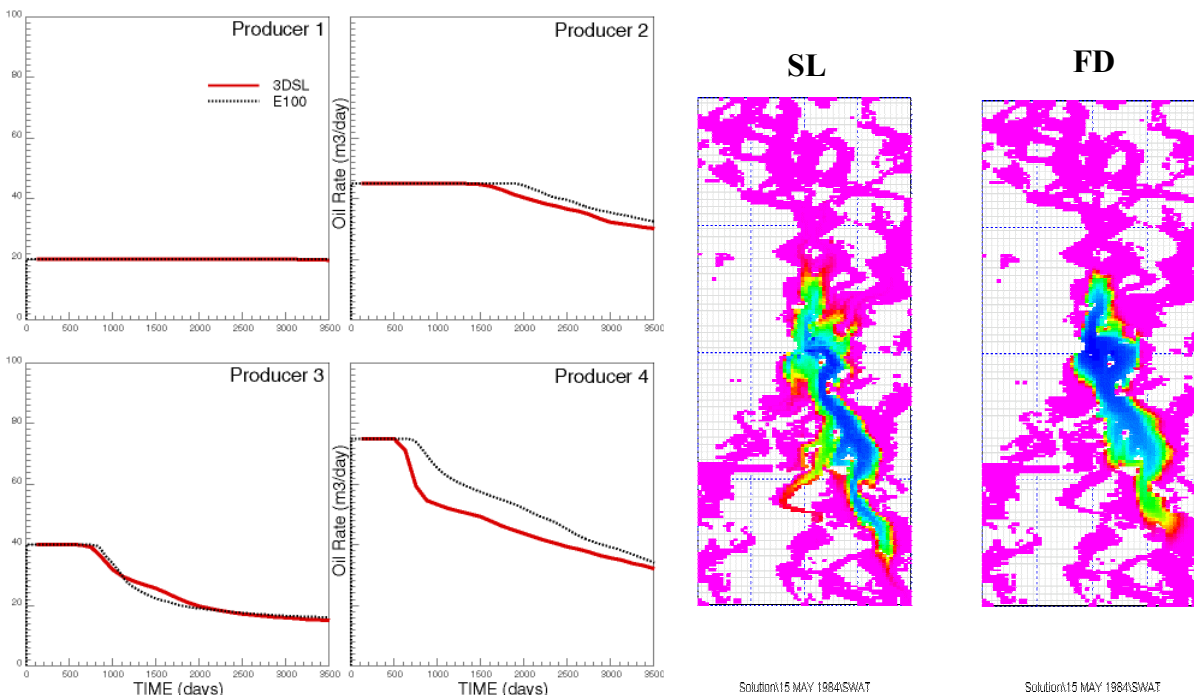


Figure 39: (left) Comparison of oil rate between SL and finite difference simulation for each producer for the 60x220x17 SP/DP model. (right) Saturation distribution prior to breakthrough in fractures for SL and FD models.

Miscible Flooding Using Streamlines

Streamlines are particularly powerful for modeling miscible gas injection and compositional simulation—these are the areas that revived the interest in streamline simulation in the first place (Emanuel *et al.* 1989, Thiele *et al.* 1995). The local sweep efficiency can be modeled accurately along each streamline while the volumetric sweep efficiency is given by the geometry of the streamlines themselves. Together, a good estimate of the overall flood performance of the entire field can be determined (Thiele *et al.* 2002). Miscible and compositional flooding are traditionally difficult

problems to solve using cell-based simulation techniques, as large fluid mobility contrasts between injected gas and resident oil in conjunction with strong permeability/porosity contrasts can lead to severe time step restrictions. The usual work around has then been to reduce the number of cells in the model at the expense of clouding the local displacement efficiency by numerical artifacts, carve out a sector of the field at expense of misrepresenting the areal sweep efficiency, and/or use simplified PVT models (Koval 1963, Todd and Longstaff 1972, Thiele et al. 2002).

Streamline simulation is generally considered a “reduced” physics approach, since the theory is framed by the assumption of fluid incompressibility, and dispersive phenomena such as capillary pressure, transverse physical dispersion, and fluid expansion are neglected. Streamline-based flow simulation therefore offers a “first-order” approximation of how a reservoir might react to gas injection. While capillary pressure, physical dispersion, and fluid compressibility are important, in many instances miscible gas injection projects are plagued by early gas breakthrough caused by reservoir heterogeneity interacting with high fluid mobility of the injected gas. In such cases, reduced physics SL simulation might offer a viable alternative to more traditional approaches, particularly when trying to evaluate the uncertainty associated with field development decisions.

In recent work, Thiele et al. (2002) used a simplified PVT model to calibrate the 1D displacement efficiency of an 8 component WAG system (N₂-C₁, CO₂-C₂, C₃-C₄, C₅-C₆, C₇-C₈, C₉-C₁₃, C₁₄-C₂₄, C₂₅+), and then used that simplified 1D solution along streamlines to model a WAG simulation of the Alpine Field in Alaska. Results were then compared to a full-physics compositional simulator. The simulations compared favorably between the two approaches (Figure 40), demonstrating that under the appropriate circumstances, SL can be used to model complex process at a fraction of the computational cost of more traditional methods.

The uncertainty in engineering WAG displacements goes beyond traditional issues associated with reservoir heterogeneity. For example, SL simulation can address more readily the number and size for WAG cycles for optimal performance, well spacing to use, or relative permeability models to use, just to mention a few. This is a good example of SL simulation as a simplified, computational efficient model, yet able to establish credible upper and lower uncertainty bounds for future development scenarios of a complex field.

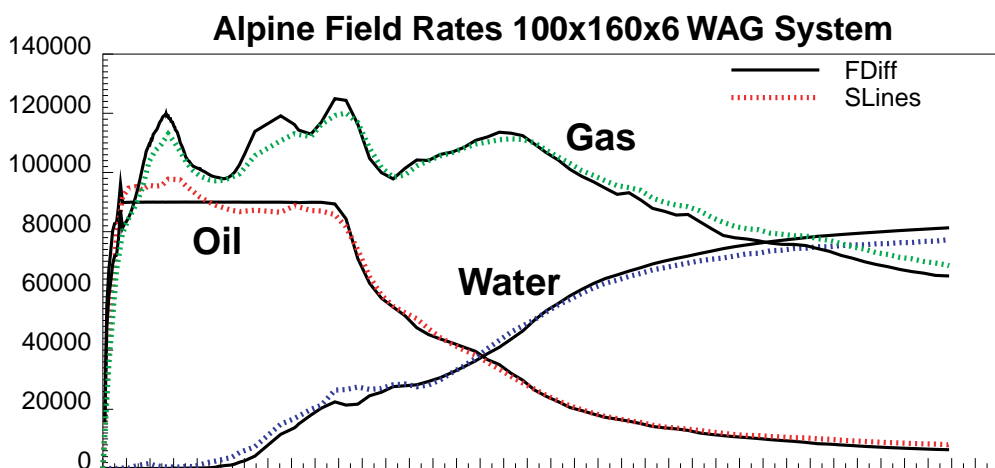


Figure 40: Field rate prediction for the Alpine Field, Alaska using a full physics compositional finite-difference model (solid) and a streamline model using a simplified PVT model (from Thiele et al. 2002).

MOVING FORWARD WITH STREAMLINE SIMULATION

Modern SL simulation is a powerful and complementary tool to traditional techniques used in engineering the upstream exploration and production of hydrocarbons. As a whole, the industry is still exploring the most optimal use of this technology and how it might be efficiently integrated into the current work flows used by individual companies and engineers. However, it is not unreasonable to expect that most companies using conventional simulation technology today will, in one form or another, use SL simulation in their future work. What remains largely unknown is if new users groups, such as geologists and geophysicists, will adopt the technology in order to bring a dynamic flow component to their analysis. What then might be expected over the next few years in terms of developments?

Compositional Simulation

The revival of modern SL simulation in the early 90's centered in part on miscible gas injection and as an alternative to the difficulties conventional methods had in resolving highly nonlinear, multiphase displacements through heterogeneous reservoirs. The numerical difficulties encountered by conventional methods for such problems continue to persist and remain a serious problem in many field-scale compositional studies. The only solution is usually to reduce the number of cells and/or reduce the geological complexity directly affecting the numerical performance. Representing the phase behavior via a more manageable number of pseudo components is the other alternative. In most cases, a combination of the two is used. But the price for these shortcuts is high. Numerical artifacts can become so severe as to completely mask any possibly beneficial phase behavior effects that might have been the reason for the numerical simulation in the first place. And going to more powerful hardware might not always yield the expected results, since run times for traditional simulation techniques can scale with a power of two or higher, quickly turning simulations into month-long computational marathons.

Streamlines remain unrivaled in the ability to efficiently transport components along flow paths, even in the presence of extreme permeability/porosity values. In the very specific case of multicomponent, multiphase flow where complex phase behavior is critical, the decoupling of the three-dimensional solution into a series of one-dimensional solutions is so attractive as a way to control numerical dispersion that it cannot be overlooked (Thiele *et al.*, 1997, Seto *et al.* 2003). For large fields under gas injection, streamlines offer advantages that will unlikely be matched by traditional technologies: the ability to model full-field scenarios with reasonable inter-well spatial resolution in acceptable run times on affordable platforms.

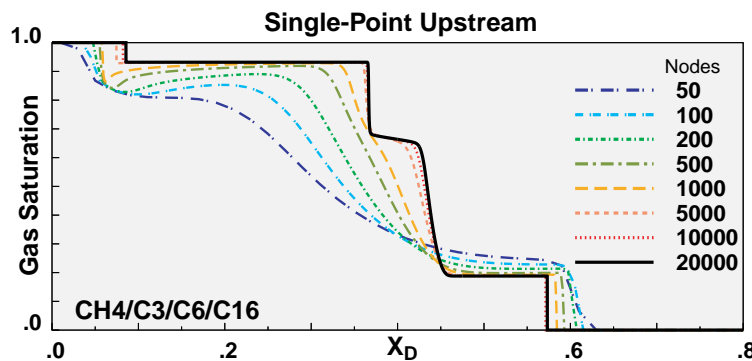


Figure 41: Four-component displacement showing that numerical diffusion remains a serious problem for field-scale reservoir simulation, where the number of gridblocks between wells is often significantly less than 50 (blue line). From Thiele & Edwards (2001).

Tracing Streamline Through Structurally Complex Reservoirs

Tracing of streamlines currently rests on Pollock's bilinear interpolation, which in turn makes the fundamental assumption that there is a single velocity per cell face. Structurally complex reservoirs, on the other hand, often require multiple connections across a single face, as might be the case in the presence of faults. This adds a layer of complexity to the tracing algorithm, since cells might now have multiple velocities across a single face, theoretically even in opposite directions. Extension to tracing of SL's in cells with multiple connections will give SL simulation the ability to model flow through heavily faulted and structurally complex systems while retaining much of its simplicity and speed. It will be an important extension to the technology and will likely allow its use for systems where traditionally more sophisticated meshing algorithms are used, such as finite-element or PEPI-grids. On-going research in this area should yield promising results within the next few years.

Streamlines in Fractured Systems

Like compositional models, dual-porosity models are computationally intensive. The work by Di Donato et al. is a clear indication that streamlines can be used for DP systems. What remains to be shown is how successfully the technology can be applied to real fields and more importantly where its limitations are. The next few years should bring a number of studies detailing the use of SL for DP systems.

Simulation of Large System

Computationally, streamlines are processed serially and completely independent of each other. This architecture lends itself perfectly to parallelization. On a multiprocessor machine or cluster of machines, the transport problem along each streamline can be computed in parallel, thereby allowing significant speed-ups. Parallelization is required for the solution of large systems, systems that might be on the order of 10^7 (or higher) gridblocks. Such systems are easily created in the case of giant oil fields (as might exist in the Middle East or Alaska) by simply allowing a reasonable block resolution between wells—25 grid blocks or more—and modeling the entire field without resorting to sector models. Even smaller reservoirs routinely have geomodels in range of 5 to 10 million cells. Large investments, both in terms hardware and software, have been made for the solution of such problems because it has been recognized that modeling the full field is critical for the engineering of optimal production scenarios. Streamlines are likely to play an important role in the future for tackling such difficult problems, particularly in assessing and screening potential scenarios for such giant models fields before resorting to more traditional approaches to confirm and cross-check a subset of the solution space.

New Work Flows

Although additional physics, such as compositional and dual porosity models, will clearly give SL simulation a larger field of applicability, the real breakthroughs for SL's are expected to come because of the integration of SL into existing and new work flows. The visualization, ease-of-use, and speed of SL's combined with novel engineering data are going to allow engineers to perform their day-to-day engineering work more efficiently and with better quality. Two of the workflows mentioned in this paper, waterflood optimization and history matching are but examples of what we can expect from SL simulation in the future. One clear area where SL simulation is likely to make a big impact is in augmenting current reservoir surveillance techniques.

The Future Simulator

Reservoir simulation is a complex field and in most instances requires expert knowledge to obtain meaningful results. Graphical user interfaces and workflows help users along and provide guidance by shielding geoscientists from some of the complexities involved. Useful and efficient

visualization of results are essential in the interpretation and validation of results. But it is a reality that the vast majority of users employ reservoir simulators as a black-box—as a transfer functions that takes a proposed reality and projects it into the future. There is little time to gain a deeper understanding of the solutions and how these are obtained. The desired is for quick answers that can be obtained relatively easy. For the simulator of the future this means that it should not be limited to a single approach: ideally it would choose which simulation technique is appropriate at what time domain and act accordingly—a “just-in-time” solution that is adequate for the solution that is currently sought. Intelligent simulators—i.e. simulators that will automatically choose the most “efficient” solution technique for the problem at hand—will likely be the focus of future development in reservoir simulation. Streamline simulation is likely to be one of the techniques the intelligent simulator of the future will have at its disposal.

ACKNOWLEDGMENTS

Ideas and results presented in this paper would not have been possible without the contribution of Rod Batycky and Martin Blunt. Their insightful and original ideas have been invaluable to the field of streamline simulation.

I would like to thank Lisette Quettier, Bernard Corre, Peter Behrenbruch, John Gardner, and Tom Schulte for their foresight and early recognition of the potential of SL simulation, and their support for the industrial development of the technology.

Many thanks to EarthDecisionSciences for the use of the GOCAD software, and to Chick Wattenbarger for GPS.

Many thanks to Darryl Fenwick and Jef Caers for the many insightful discussions on SL aided history matching, and the Herve Gross for being a catalyst for the Stanford/Streamsim consortium on streamline-aided history matching.

Many thanks to Anadarko, Apache, ConocoPhillips, ENI, Saudi Aramco, and Total for supporting the Stanford/Streamsim consortium on streamline-aided history matching.

The author would like to thank the members of the ITF project in association with Imperial College for supporting the streamline-based dual-porosity efforts.

Thanks to Michael Edwards for his discussions on the AIM method used in DP systems and Darryl Fenwick for his assistance with the flow simulations for the SPE10 upscaled DP model.

REFERENCES

1. 3DSL, User Manual v2.20, Feb 2005, Streamsim Technologies.
2. Agarwal, B. and Blunt, M.J.: “A Full-Physics, Streamline-Based Method for History Matching Performance Data of a North Sea Field,” paper SPE 66388 in proceedings of the Reservoir Simulation Symposium, Houston, TX (February 2001).
3. Agarwal, B. and Blunt, M.J.: “A Streamline-Based Method for Assisted History Matching Applied to an Arabian Gulf Field,” *SPE Journal* (December 2004) 437-449.
4. Al-Huthali, A. H. and Datta-Gupta, A.: “Streamline simulation of water injection in naturally fractured reservoirs,” SPE 89443, proceedings of the SPE/DOE Symposium on Improved Oil Recovery, Tulsa, OK, 17-21 April (2004).
5. Batycky, R.P.: “A Three-Dimensional Two-Phase Field Scale Streamline Simulator,” PhD Thesis, Stanford University, Dept. of Petroleum Engineering, Stanford, CA, 1997.

6. Batycky, R.P., Blunt, M.J., and Thiele, M.R.: "A 3D Field Scale Streamline-Based Reservoir Simulator," *SPE Reservoir Engineering* (November 1997) 246-254.
7. Baker, R., Kuppe, F., Chug, S., Bora, R., Stojanovic, S., and Batycky, R.P.: "Full-Field Modeling Using Streamline-Based Simulation: 4 Case Studies" *SPEE* (2002) 5(2), 126-134.
8. Blunt, M.J., Liu, K., and Thiele, M.R.: "A Generalized Streamline Method to Predict Reservoir Flow," *Petroleum Geoscience*, Vol. 2, 256-269, 1996.
9. Bommer, M.P. and Schechter, R.S.: "Mathematical Modeling of In-Situ Uranium Leaching," *SPEJ* (December 1979) 19, 393-400.
10. Bratvedt, F., Gimse, T. and Tegnander, C.: "Streamline computations for porous media flow including gravity." *Transport in Porous Media*, Vol. 25, No. 1, 63-78 (Oct. 1996).
11. Bratvedt, F., Bratvedt, K., Buchholz, C., Holden, L., Holden, H., and N.H. Risebro: "A New Front-Tracking Method for Reservoir Simulator," *SPE Reservoir Engineering* (February 1992) 107-116. Caers, J. "Primer on Geostatistics" to appear in 2005. Caers, J. "Efficient Gradual Deformation Using a Streamline-Based Proxy Method" *Journal of Petroleum Science and Engineering*, 39, 2003, 57-83. Caers, J., Krishnan, S., Wang, Y. & Kovscek, A. R.: "A Geostatistical Approach to Streamline-based History Matching" *SPE Journal*. 7(3) September 2002, 250-266.
15. Castellini, A., Edwards, M.G. and Durlofsky, L.J., 'Flow Based Modules for grid Generation in two and Three Dimensions', Proc. 7th European Conference on the Mathematics of Oil Recovery, Baveno, Italy, 2000.
16. Christie, M.A. and Blunt, M.J.: "Tenth SPE Comparative Solution Project: A Comparison of Upscaling Techniques," *SPE Reservoir Evaluation & Engineering* (August 2001) 308-317.
17. Christie, M.A. and Clifford, P.J.: "A Fast Procedure for Upscaling in Compositional Simulation," paper SPE 37986 in proceedings of the 1997 SPE Reservoir Simulation Symposium, Houston, TX (Jun. 1997).
18. Christie, M.A., Subbey, S., Sambridge, M., and Thiele, M.: "Quantifying Prediction Uncertainty in Reservoir Modelling Using Streamline," paper presented at the 15th ASCE Engineering Mechanics Conference, June 2-5, 2002.
19. Cordes, C. and Kinzelbach, W., 'Continuous Groundwater Velocity Fields and Path Lines in Linear, Bilinear and Trilinear Finite Elements', *Water Resources. Res.*, 30(4), 965-973, 1994.
20. Datta-Gupta, A. and King, M.J.: "A Semi-Analytic Approach to Tracer Flow Modeling in Heterogeneous Permeable Media," *Advances in Water Resources* (1995) 18(1), 9-24.
21. Di Donato, G., Huang, W., and Blunt, M.J.: "Streamline-Based Dual Porosity Simulation of Fractured Reservoirs," SPE 84036 proceedings of the SPE Annual Technical Conference and Exhibition Denver, Colorado, U.S.A., 5 - 8 October 2003.
22. Di Donato, G. and Blunt, M.J.: "Streamline-based dual-porosity simulation of reactive transport and flow in fractured reservoirs," *Water Resources Research*, 40, W04203, doi:10.1029/2003WR002772 (2004).
23. Emanuel, A.S., Alameda, G.K., Behrens, R.A., and Hewett, T.A.: "Reservoir Performance Prediction Methods on Fractal Geostatistics," *SPE Reservoir Engineering* (August 1989) 311-318.

24. Emanuel, A.S. and Milliken, W.J.: “Application of Streamtube Techniques to Full-Field Waterflooding Simulation,” SPE (August 1997), 211-217.
25. Emanuel, A.S. and Milliken, W.J.: “Application of 3D Streamline Simulation to Assist History Matching,” SPE paper 49000 in proceedings of the 1998 ATCE, New Orleans, LA (October).
26. floodOPT, User Manual v0.6, February 2005, Streamsim Technologies.
27. Glimm, J. *et al*, “Front Tracking Reservoir Simulator, Five-Spot Validation Studies and the Water Coning Problem,” *The Mathematics of Reservoir Simulation*, R. Ewing (Ed.), SIAM, Philadelphia (1983) 107-36.
28. Gilman J.R. and Kazemi, H.: “Improvement in Simulation of Naturally Fractured Reservoirs,” SPEJ, September 1983, Vol. 23, 695-707.
29. Gilman, J.R., Meng, H.-Z., Uland, M.J., Dzurman, P.J., Cosic, S., “Statistical Ranking of Stochastic Geomodels Using Streamline Simulation: A Field Application,” SPE 77374 presented at the SPE Annual Technical Conference & Exhibition, San Antonio, TX 29 Sept - 2 Oct., 2002.
30. Ingebrigtsen, L., Bratvedt, F. and Berge, J.: “A Streamline Based Approach to Solution of Three-Phase Flow”, SPE 51904 in proceedings of the SPE Reservoir Simulation Symposium, Houston, TX, 14-17 February 1999.
31. Kazemi, H., Gilman, J.R., and Eisharkawy, A.A.: “Analytical and Numerical Solution of Oil Recovery From Fractured Reservoirs With Empirical Transfer Functions,” SPE Reservoir Engineering, May 1992, Vol. 6, 219-227.
32. King, M. J. and Datta-Gupta, A.: ‘Streamline Simulation: A Current Perspective’, *In Situ*, 22(1): 91-140, 1998.
33. King, M.J., Blunt, M.J., Mansfield, M., and Christie, M.A.: ‘Rapid Evaluation of the Impact of Heterogeneity on Miscible Gas Injection,’ paper SPE26079 in proceedings of the Western Regional Meeting, Anchorage, AK (1993).
34. Koval, E.J.: “A Method for Predicting the Performance of Unstable Miscible Displacements in Heterogeneous Media,” *Society of Petroleum Engineers Journal* (June 1963) 145-154.
35. Le Ravalec-Dupin, M. and Fenwick, D.H.: “A Combined Geostatistical and Streamline-Based History Matching Procedure,” paper SPE77378 in proceedings of the 2002 ATCE, San Antonio, TX, 29 Sept.–2 Oct. 2002.
36. Lolomari, T., Bratvedt, K., Crane, M., and Milliken, W.: “The Use of Streamline Simulation in Reservoir Management: Methodology and Case Studies,” paper SPE63157 in proceedings of the 2000 ATCE, Dallas, TX (October).
37. Manceau, E., Mezghani, M., Zabalza-Mezghani, and Roggero, F.: “Combination of Experimental Design and Joint Modeling Methods for Quantifying the Risk Associated with Deterministic and Stochastic Uncertainties—An Integrated Test Study,” paper SPE71620 presented at the 2001 ATCE, New Orleans Sept. 30 – Oct. 3.
38. Martin, J.C. and Wegner, R.E.: “Numerical Solution of Multiphase, Two-Dimensional Incompressible Flow Using Streamtube Relationships” *Society of Petroleum Engineers Journal* (October 1979) 19, 313-323.
39. Mlacnik, M.J., Durllofsky, L.J., and Heinemann, Z.E.: “Dynamic Flow-Based PEBI Grids for Reservoir Simulation” paper SPE90009 presented at the 2004 ATCE, Houston, TX, Sept. 26-29.

40. Muskat, M. and Wyckoff, R.: "Theoretical Analysis of Waterflooding Networks," *Trans. AIME* (1934) 107, 62-77.
41. Pollock, D.W.: "Semianalytical Computation of Path Lines for Finite-Difference Models," *Ground Water*, (November-December 1988) 26(6), 743-750.
42. Portella, R.C.M. and Hewett, T.A.: "Upscaling, Gridding, and Simulating Using Streamtubes," *Society of Petroleum Engineers Journal* (September 2000) 5 (3), 315-323.
43. Prévost, M., Edwards, M.G., and Blunt, M.J.: "Streamline Tracing on Curvilinear Structured and Unstructured Grids," *SPE Journal* 7(2) 139-148, June (2002).
44. Renard, G.: "A 2D Reservoir Streamtube EOR Model with Periodic Automatic Regeneration of Streamlines," *In Situ* (1990) 14, No. 2, 175-200.
45. Samier, P., Quettier, L., and Thiele, M.: "Applications of Streamline Simulations to Reservoir Studies," *SPEE* (2002) 5(4), 324-332.
46. Schulze-Riegert, R.W., J.K. Axmann, Haase, O., Rian, D.T., and You Y.-L., "Evolutionary Algorithms Applied to History Matching of Complex Reservoirs," *SPE Reservoir Evaluation & Engineering* (April 2003) 163-173.
47. Seto, C.J., Jessen, K., Orr, F.M. Jr.: "Compositional Streamline Simulation of Field Scale Condensate Vaporization by Gas Injection," paper SPE 79690 in proceedings of the 2003 SPE Reservoir Simulation Symposium, Houston, TX (Feb. 2003).
48. Stüben, K.: Algebraic Multigrid (AMG): An Introduction with Applications. Guest appendix in the book "Multigrid" by U. Trottenberg; C.W. Oosterlee; A. Schüller. Academic Press, 2000.
49. Strebelle, S., Payrzyan, K., and Caers, J., "Modeling of a Deepwater Turbidite Reservoir Conditional to Seismic Data Using Multiple-Point Geostatistics," SPE 77425 presented at the SPE Annual Technical Conference & Exhibition, San Antonio, TX 29 Sept - 2 Oct., 2002.
50. Thiele, M.R., Blunt, M.J., and Orr, F.M.: "Modeling Flow in Heterogenous Media Using Streamtubes—II. Compositional Displacements," *InSitu* (November 1995) 19, No. 4, 367.
51. Thiele, M.R., Batycky, R.P., Blunt, M.J., and Orr, F.M.: "Simulating Flow in Heterogeneous Media Using Streamtubes and Streamlines," *SPE Reservoir Engineering* (February 1996) 10, No. 1, 5-12.
52. Thiele, M.R., Batycky, R.P., and Blunt, M.J.: "A Streamline Based 3D Field-Scale Compositional Reservoir Simulator," SPE paper #38889 in proceedings of the 1997 ATCE, San Antonio, TX (October).
53. Thiele, M.R. and Batycky, R.P.: "Discussion of SPE65604—Streamline Simulation: A Technology Update," *Journal of Petroleum Technology* (May 2001), 53, No.5, 26-27
54. Thiele, M.R. and Edwards, M.G.: "Physically Based Higher-Order Godunov Schemes for Compositional Simulation," paper SPE 66403 in proceedings of the 2001 SPE Reservoir Simulation Symposium, Houston, TX (Feb. 2001).
55. Thiele, M.R., Batycky R.P., and Kent, L.T.: "Miscible WAG Simulations Using Streamlines," in proceedings of the 8th European Conference on the Mathematics of Oil Recovery (ECMOR), Freiberg, Germany, 3-6 Sept., 2002.
56. Thiele, M.R. and Batycky, R.P.: "Water Injection Optimization of a Giant Carbonate Field Using a Streamline-Based Workflow," SPE 84080 in proceedings of the SPE ATCE, Denver, CO, 5-8 October 2003.

57. Thiele, M.R., Batycky, R.P., Iding, M., and Blunt, M.J.: “Extension of Streamline-Based Dual Porosity Flow Simulation to Realistic Geology,” in proceedings of the 9th European Conference on the Mathematics of Oil Recovery (ECMOR), Cannes, France, 30th Aug. -2nd Sept., 2004.
58. Todd, M.R. and Longstaff, W.J.: “The Development, Testing, and Application of a Numerical Simulator for Predicting Miscible Flood Performance,” *Journal of Petroleum Technology* (July 1972) 874-882.
59. Vasco, D.W., Yoon, S., and Datta-Gupta, A.: “Integrating Dynamic Data into High-Resolution Reservoir Models Using Streamline-Based Analytical Sensitivity Coefficients,” *SPE Journal* (4) 389-399 (1999).
60. Wang, Y. and Kovscek, A.R.: “Streamline Approach for History Matching Production Data,” *SPE Journal* (4), 353-362, (December 2000).
61. Wen X.-H., Deutsch, C.V., and Cullick, A.S.: “A Fast Streamline-Based Method for Computing Sensitivity Coefficients for Fractional Flow Rate,” SPE paper 50693 in proceedings of the 1998 ATCE, New Orleans, LA (October).
62. White, C.D., Willis, B.J., Narayanan, K., and Dutton, S.P.: “Identifying and Estimating Significant Geological Parameters with Experimental Design,” *SPE Journal* (6), 311-324, (September 2001).
63. Williams, G.J.J., Mansfield, M., MacDonald, G., and Bush, M.D.: “Top-Down Reservoir Modeling,” SPE paper 89974 in proceedings of the 2004 ATCE, Houston, TX (26-29 Sept.).